Deficiency of primate-specific *SSX1* induced asthenoteratozoospermia in infertile men and cynomolgus monkey and tree shrew models

Authors

Chunyu Liu, Wei Si, Chaofeng Tu, ..., Yue-Qiu Tan, Yunxia Cao, Feng Zhang

Correspondence

caoyunxia6@126.com (Y.C.),
zhangfeng@fudan.edu.cn (F.Z.)

The importance of primate-specific genes (PSGs) in spermatogenesis is largely unknown. This study identified variants in an X-linked PSG, *SSX1*, associated with male infertility. By using cynomolgus monkey and tree shrew models, this study provides a powerful experimental system for elucidating the functions of testis-enriched PSGs in spermatogenesis.

Liu et al., 2023, The American Journal of Human Genetics *110*, 516–530
March 2, 2023

https://doi.org/10.1016/j.ajhg.2023.01.016

CellPress

ARTICLE

Deficiency of primate-specific *SSX1* induced asthenoteratozoospermia in infertile men and cynomolgus monkey and tree shrew models

Chunyu Liu,[1,2,25] Wei Si,[3,25] Chaofeng Tu,[4,5,25] Shixiong Tian,[6,7,25] Xiaojin He,[8,9,10,25] Shengnan Wang,[3,25] Xiaoyu Yang,[11,25] Chencheng Yao,[12,13,25] Cong Li,[14] Zine-Eddine Kherraf,[15,16] Maosen Ye,[17,18] Zixue Zhou,[7] Yuhua Ma,[19] Yang Gao,[8,9] Yu Li,[17,18] Qiwei Liu,[3] Shuyan Tang,[1,2] Jiaxiong Wang,[20] Hexige Saiyin,[1] Liangyu Zhao,[21] Liqun Yang,[14,22] Lanlan Meng,[4,5] Bingbing Chen,[3] Dongdong Tang,[8,9,10] Yiling Zhou,[1,2] Huan Wu,[8,9,10] Mingrong Lv,[8,9,10] Chen Tan,[4] Ge Lin,[4,5] Qingpeng Kong,[14,22] Hong Shi,[3] Zhixi Su,[23] Zheng Li,[12,13] Yong-Gang Yao,[17,18,19,24] Li Jin,[1,7] Ping Zheng,[14,17,19] Pierre F. Ray,[15,16] Yue-Qiu Tan,[4,5,26] Yunxia Cao,[8,9,10,26,*] and Feng Zhang[1,2,7,26,*]

Summary

Primate-specific genes (PSGs) tend to be expressed in the brain and testis. This phenomenon is consistent with brain evolution in primates but is seemingly contradictory to the similarity of spermatogenesis among mammals. Here, using whole-exome sequencing, we identified deleterious variants of X-linked *SSX1* in six unrelated men with asthenoteratozoospermia. *SSX1* is a PSG expressed predominantly in the testis, and the *SSX* family evolutionarily expanded independently in rodents and primates. As the mouse model could not be used for studying *SSX1*, we used a non-human primate model and tree shrews, which are phylogenetically similar to primates, to knock down (KD) *Ssx1* expression in the testes. Consistent with the phenotype observed in humans, both *Ssx1*-KD models exhibited a reduced sperm motility and abnormal sperm morphology. Further, RNA sequencing indicated that *Ssx1* deficiency influenced multiple biological processes during spermatogenesis. Collectively, our experimental observations in humans and cynomolgus monkey and tree shrew models highlight the crucial role of *SSX1* in spermatogenesis. Notably, three of the five couples who underwent intra-cytoplasmic sperm injection treatment achieved a successful pregnancy. This study provides important guidance for genetic counseling and clinical diagnosis and, significantly, describes the approaches for elucidating the functions of testis-enriched PSGs in spermatogenesis.

Introduction

Infertility has become a growing medical problem, and according to large population surveys, it affects at least 180 million people worldwide.[1] Idiopathic sperm abnormalities, which are direct causes of infertility in males, account for approximately 30% of individuals with male infertility.[2] Asthenoteratozoospermia, a form of sperm abnormality, has been defined as a disorder with a significant genetic contribution.[3] Previous strategies for exploring

[1]Obstetrics and Gynecology Hospital, State Key Laboratory of Genetic Engineering, School of Life Sciences, Institute of Reproduction and Development, Fudan University, Shanghai, China; [2]Shanghai Key Laboratory of Female Reproductive Endocrine Related Diseases, Fudan University, Shanghai, China; [3]State Key Laboratory of Primate Biomedical Research, Institute of Primate Translational Medicine, Kunming University of Science and Technology, Kunming, China; [4]Institute of Reproductive and Stem Cell Engineering, NHC Key Laboratory of Human Stem Cell and Reproductive Engineering, School of Basic Medical Science, Central South University, Changsha, China; [5]Clinical Research Center for Reproduction and Genetics in Hunan Province, Reproductive and Genetic Hospital of CITIC-Xiangya, Changsha, China; [6]Shanghai Key Laboratory of Metabolic Remodeling and Health, Institute of Metabolism and Integrative Biology, Fudan University, Shanghai, China; [7]Human Phenome Institute, Zhangjiang Fudan International Innovation Center, Fudan University, Shanghai, China; [8]Reproductive Medicine Center, Department of Obstetrics and Gynecology, The First Affiliated Hospital of Anhui Medical University, Hefei, China; [9]NHC Key Laboratory of Study on Abnormal Gametes and Reproductive Tract, Anhui Medical University, Hefei, China; [10]Key Laboratory of Population Health Across Life Cycle, Anhui Medical University, Ministry of Education of the People's Republic of China, Hefei, China; [11]State Key Laboratory of Reproductive Medicine, Clinical Center for Reproductive Medicine, The First Affiliated Hospital of Nanjing Medical University, Nanjing, China; [12]Department of Andrology, Center for Men's Health, Urologic Medical Center, Shanghai General Hospital, Shanghai Jiao Tong University School of Medicine, Shanghai, China; [13]Shanghai Key Lab of Reproductive Medicine, Shanghai Jiao Tong University School of Medicine, Shanghai, China; [14]State Key Laboratory of Genetic Resources and Evolution, Kunming Institute of Zoology, Chinese Academy of Sciences, Kunming, China; [15]Université Grenoble Alpes, INSERM U1209, CNRS UMR 5309, Institute for Advanced Biosciences, Team Genetics Epigenetics and Therapies of Infertility, Grenoble, France; [16]CHU Grenoble Alpes, UM GI-DPI, Grenoble, France; [17]Key Laboratory of Animal Models and Human Disease Mechanisms of the Chinese Academy of Sciences & Yunnan Province, and KIZ-CUHK Joint Laboratory of Bioresources and Molecular Research in Common Diseases, Kunming Institute of Zoology, Chinese Academy of Sciences, Kunming, China; [18]Kunming College of Life Science, University of Chinese Academy of Sciences, Kunming, China; [19]National Resource Center for Non-Human Primates, National Research Facility for Phenotypic & Genetic Analysis of Model Animals (Primate Facility), Kunming Institute of Zoology, Chinese Academy of Sciences, Kunming, China; [20]Center for Reproduction and Genetics, State Key Laboratory of Reproductive Medicine, The Affiliated Suzhou Hospital of Nanjing Medical University, Suzhou Municipal Hospital, Suzhou, China; [21]The Fifth Affiliated Hospital of Sun Yat-sen University, Zhuhai, China; [22]Key Laboratory of Healthy Aging Research of Yunnan Province, Kunming Institute of Zoology, Chinese Academy of Sciences, Kunming, China; [23]Singlera Genomics (Shanghai) Limited, Shanghai, China; [24]Center for Excellence in Brain Science and Intelligence Technology, Chinese Academy of Sciences, Shanghai, China
[25]These authors contributed equally
[26]These authors contributed equally
*Correspondence: caoyunxia6@126.com (Y.C.), zhangfeng@fudan.edu.cn (F.Z.)
https://doi.org/10.1016/j.ajhg.2023.01.016.

genetic factors related to asthenoteratozoospermia have mainly relied on the identification of genetic defects commonly shared by multiple affected individuals.[4,5] However, human evidence alone based on a common genetic defect among individuals is not enough for proving a pathogenic genetic factor. The use of appropriate model organisms may provide further reliable functional evidence for the genotype-phenotype correlation and facilitate studies on the molecular mechanisms underlying male infertility.[6]

Mice have been widely used as a model organism in studies on genetic disorders.[7–9] However, for studies on human mutated genes that are not evolutionarily conserved between mice and humans, a mouse model is not applicable because of the lack of one-to-one mouse orthologs for genetic manipulation and subsequent phenotypic analysis. A recent study on the human genome identified more than 800 primate-specific genes (PSGs), more than 30% of which are predominantly expressed in the testis.[10] A similar pattern was also clearly observed with ampliconic genes on the human X chromosome; 69% of these genes have no orthologs in mice, and the majority of them are expressed predominantly or specifically in testicular germ cells.[11,12] Therefore, new model organisms are needed to study the potential spermatogenic functions of testis-enriched PSGs and their genetic contributions to male infertility.

As a non-human primate model, cynomolgus monkeys share high similarities with humans in terms of both genetic and physiological characteristics and have been used for modeling human neurodegenerative and cognitive diseases as well as complex behaviors.[13] However, the generation of gene-edited offspring and subsequent reproductive phenotyping in adult monkeys take approximately 4–5 years because of long breeding cycles. Instead, *in vivo* genetic manipulation with adeno-associated virus (AAV) and short hairpin RNA (shRNA) can facilitate short-term observations on genetically related phenotypes. Furthermore, tree shrews are close relatives to primates because of their high degree of similarities in both molecular and physiological aspects.[14,15] Moreover, recent studies successively revealed the reference genomes for tree shrews.[14,16–18] For PSGs, the orthologs in tree shrews have more similarities than these identified in mice. Therefore, cynomolgus monkeys and tree shrews may be used as promising model organisms for genetic manipulation in the testis and studying the functions of PSGs in spermatogenesis.

Here, we identified deleterious variants of X-linked PSG *SSX1* (MIM: 312820) as a factor for asthenoteratozoospermia. Furthermore, we achieved *Ssx1* testicular knockdown (*Ssx1*-KD) models by injecting AAV9-*Ssx1*-shRNA vectors into the seminiferous tubules in the testes of adult male cynomolgus monkeys and tree shrews. Notably, both *Ssx1*-KD models mimicked the asthenoteratozoospermia phenotypes observed in humans. Interestingly, our bioinformatics analysis revealed that over 1,000 human testis-enriched genes do not have one-to-one orthologs in mice or that their murine orthologs are not testis-enriched, highlighting the need to develop animal models that are phylogenetically closer to human. This study provides a powerful system for the genetic manipulation of germ cells in the testes of cynomolgus monkey and tree shrew models. The described strategy could be used for elucidating the functions of hundreds of testis-enriched PSGs in spermatogenesis.

Material and methods

Cohort description

In total, a cohort of 536 Chinese infertile men affected by asthenoteratozoospermia were enrolled from the First Affiliated Hospital of Anhui Medical University, the Reproductive and Genetic Hospital of CITIC-Xiangya (Changsha), and the First Affiliated Hospital of Nanjing Medical University in China. All the recruited subjects presented with primary infertility accompanied by a variety of abnormal sperm morphologies. Clinical investigation revealed that all the subjects in this study displayed normal male external genitalia, bilateral testicular sizes, hormone levels, and secondary sexual characteristics. The chromosomal karyotypes of all the individuals were also normal (46; XY), and no large-scale deletions were observed in the Y chromosome. This study was approved by the institutional review boards of all the participating institutes. Signed informed consent was obtained from all the subjects who participated in the study.

Whole-exome sequencing (WES)

DNA samples for WES were prepared and sequenced according to a previously described protocol.[19] Briefly, genomic DNA was isolated from the peripheral blood samples of human subjects via a DNeasy Blood and Tissue Kit (Qiagen, 51106). Then, we used 1 μg of genomic DNA to enrich the human exome by using the AIExome Enrichment Kit V2 (iGeneTech, China), and we conducted next-generation sequencing with the NovaSeq 6000 platform (Illumina, San Diego, CA). The obtained raw data were mapped to the human genome reference assembly (GRCh37/hg19) with Burrows-Wheeler Aligner (BWA) software, and PCR duplicates were marked and removed via Picard software.[20] ANNOVAR software was used for functional annotation with information from OMIM, Gene Ontology, KEGG Pathway, SIFT, PolyPhen-2, MutationTaster, 1000 Genomes Project, and gnomAD.[21–25] According the incidence rates of asthenoteratozoospermia in human populations, genetic variants with allele frequencies ≥ 0.01 in the human population genome datasets (e.g., the gnomAD browser and 1000 Genomes Project) were filtered out. Nonsense, frameshift, and essential splice-site variants were preferred. Missense variants that were predicted to be deleterious by bioinformatic tools were also included for further evaluation. Sanger sequencing was performed for variant verification with the primers listed in Table S1.

Semen parameter analysis

Semen analyses were carried out in source laboratories during routine biological examinations of the individuals according to the WHO guidelines.[26] Semen samples from the infertile men were collected by masturbation after 2–7 days of sexual abstinence, and the samples were evaluated after liquefaction for 30 min at 37°C. We assessed sperm morphology with hematoxylin and eosin (H&E) staining and scanning electron microscopy

(SEM), and we examined at least 200 spermatozoa to evaluate the rates of abnormal sperm morphologies for each subject.

For semen analyses for cynomolgus monkeys, semen samples were acquired by penile electroejaculation before AAV9-*Ssx1*-shRNA or AAV9-NC-shRNA vectors injection and at 45, 60, and 75 days after injection. For morphology and motility analyses of tree shrew sperm, spermatozoa were extracted from the cauda epididymides through dissection of adult male tree shrews, diluted in 1 mL of HEPES-TL (Cat. # IVL01-10201007, Caisson Labs), and incubated for 15 min at 37°C. Sperm morphologies of cynomolgus monkeys and tree shrews were also analyzed by H&E staining and SEM, and sperm motility was assessed by a CASA system.

Establishment of cynomolgus monkey and tree shrew models

Production of AAV vectors

A previous study indicated that AAV9, one of 12 serotypes (AAV1–AAV12), can penetrate not only the blood-testis barrier (BTB) but also the basement membrane of the seminiferous tubules.[27] To KD the expression of *Ssx1* in the testes of cynomolgus monkeys and tree shrews, AAV9 vectors containing shRNA were provided by Hanbio Biotechnology (Shanghai, China), and we used these to target the specific sequences of *Ssx1*. Briefly, *Ssx1*-shRNAs and control-shRNA were designed, synthesized, and cloned into the pHBAAV-U6-MCS-CMV-EGFP vectors. Then, we cotransfected the vectors with *Ssx1* overexpression plasmids into HEK293T cells by using Lipofectamine 2000 reagent for 48 h. We performed subsequent real time qPCR analysis to validate the KD efficacy of the shRNAs (Figure S1). We used the plasmids of the most efficient shRNAs (Table S2) to package AAV9 virus (Hanbio) for the *in vivo* KD of *Ssx1*. In addition, to investigate the possible targeting of the selected *Ssx1*-shRNAs for other *Ssx* family members, we also cotransfected selected *Ssx1*-shRNAs with overexpression plasmids of other *Ssx* family members into HEK293T cells, and we also detected the KD efficacy by real-time qPCR analysis (Figure S2).

Injection of AAV9-Ssx1-shRNA or AAV9-NC-shRNA vectors into the testes

To KD *Ssx1* in cynomolgus monkeys, four adult male cynomolgus monkeys (*Macaca fascicularis*) were provided by the State Key Laboratory of Primate Biomedical Research (Kunming, China). One cynomolgus monkey was designated as the NC (negative control) group, and the other three cynomolgus monkeys were designated as the *Ssx1*-KD group. The cynomolgus monkey testes were examined under an ultrasound (LOGIQ P5/A5, GE Healthcare, USA), and the testicular reticulum showed a linear echo dense structure. Then, a needle bevel was punctured into the rete of testicular tissue under the guide of ultrasound and 1 mL of CM-AAV9-NC-shRNA solution or CM-AAV9-*Ssx1*-shRNA solution (a dose of 1.4×10^{12} vector genome/mL) was injected from the rete testis space and scattered to the seminiferous tubules. Sperm samples were collected from male cynomolgus monkeys by penile electroejaculation[28] before injection and at 45, 60, and 75 days after injection. Testicular tissues were obtained by puncture for further functional analyses. All the experimental procedures were approved by the Institutional Animal Care and Use Committee of Kunming University of Science and Technology (authorization code: LPBR201701001) and were performed in accordance with the Guide for Care and Use of Laboratory Animals.[29]

For the KD of *Ssx1* in tree shrews, a total of 15 wild-type adult (6 months or older) male Chinese tree shrews (*Tupaia belangeri chinensis*) were provided by the Kunming Primate Research Center in Kunming Institute of Zoology, Chinese Academy of Sciences. To KD *Ssx1* in the testes of tree shrews, each adult tree shrew was injected with 80 μL of TR-AAV9-NC-shRNA solution (nontargeting control) or TR-AAV9-*Ssx1*-shRNA solution (a dose of 1.5×10^{12} vector genome/mL) into the seminiferous tubules of bilateral testes through the rete testis. For each solution, approximately 0.4% Trypan blue tracer was added to monitor the injection. Then, tree shrews were sacrificed on the 60th day post injection, and testis tissues and epididymal effluents were collected for further phenotypic analyses. All the experimental and animal care procedures were performed according to the protocols approved by the Institutional Animal Care and Use Committee of the Kunming Institute of Zoology, Chinese Academy of Sciences.

Electron microscopy evaluation

Sperm samples obtained from men and male cynomolgus monkeys and tree shrews were fixed with 2.5% glutaraldehyde for 24 h at 4°C before electron microscopy evaluation. For transmission electron microscopy (TEM), sperm cells were washed and postfixed with 1% osmium tetroxide in 0.1 mol/L PB for 1–1.5 h at 4°C. Then, dehydration was performed with graded ethanol (50%, 70%, 90%, and 100%) and 100% acetone solutions, followed by infiltration with 1:1 acetone and SPI-Chem resin (containing dodecenyl succinic anhydride, N-methylacetamide, SPI-Pon 812, and DMP-30) overnight at 37°C. After infiltration and embedding in Epon 812, the specimens were sliced with an ultramicrotome, stained with uranyl acetate and lead citrate, and then observed and photographed via TEM (TECNAI-10, Philips) with an accelerating voltage of 80 kV.

For the SEM assay, after being deposited on poly-L-lysine-coated coverslips, sperm specimens were fixed in 2.5% glutaraldehyde, washed with 0.1 mol/L phosphate buffer, and postfixed in osmic acid. Then, the samples were progressively dehydrated with an ethanol and isoamyl acetate gradient and dried with a CO_2 critical-point drier (Eiko HCP-2, Hitachi). Next, the specimens were mounted on aluminum stubs, sputter-coated with an ionic sprayer meter (Eiko E-1020, Hitachi), and analyzed via SEM (Stereoscan 260) under an accelerating voltage of 20 kV.

Real-time qPCR and immunoblotting analyses

Total RNA and protein were extracted from human spermatozoa or testicular tissues of cynomolgus monkeys and tree shrews via the Allprep DNA/RNA/Protein Mini Kit (Qiagen) according to the manufacturer's instructions. For real-time qPCR, 1 μg of total RNA was converted into cDNA with HiScript II Q RT Super-Mix for qPCR (Vazyme). Then, the obtained cDNAs were individually diluted by 5-fold to be used as templates for the subsequent real-time fluorescence qPCR, which was performed with AceQ qPCR SYBR Green Master Mix (Vazyme) on a CFX Connect Real-Time PCR Detection System. *GAPDH* and *β-actin* were used as the internal controls. The primer sequences used for real-time qPCR are presented in Tables S3 and S4.

For immunoblotting analysis, the protein samples were denatured at 95°C for 10 min, separated with 10% SDS-polyacrylamide gels, and transferred to polyvinylidene difluoride (PVDF) membranes (Millipore). Then, the membranes were blocked for 1 h with 5% nonfat milk at room temperature and incubated with primary antibodies (SSX1, PA5-61070, Invitrogen, 1:1,000; CCDC39, HPA035364, Sigma, 1:1,000; CEP44, A8317, ABclonal, 1:1,000; DPY19L2, bs-8291R, Bioss, 1:1,000; KIFAP3, A4518,

ABclonal, 1:1,000; NR4A2, A22011, ABclonal, 1:1,000; SMURF2, A10592, ABclonal, 1:1,000; TAF5, A7221, ABclonal, 1:1,000; UPF2, A13411, ABclonal, 1:1,000; HRP-conjugated beta actin, HRP-60008, Proteintech, 1:2,000) overnight at 4°C, respectively. After being washed with TBST and incubated with HRP-conjugated secondary antibody (M21002, Abmart, 1:4,000) for 1 h at room temperature, the PVDF membranes were visualized with Chemistar High-sig ECL Western Blotting Substrate (Tanon) by Tanon 5200.

Immunofluorescence (IF) analysis

IF analyses were performed on spermatozoa from human individuals and testicular tissues from tree shrews. For IF analysis of sperm cells, semen samples (fixed in 4% paraformaldehyde at least 24 h) were deposited on slides that were precoated with 0.1% poly-L-lysine (Thermo Fisher Scientific) before being washed two times with PBS and blocked in 10% donkey serum for 1 h at room temperature. Then, the slides were subsequently incubated overnight at 4°C with the following primary antibodies: rabbit polyclonal anti-SSX1 (PA5-61070, Invitrogen, 1:200) and mouse monoclonal anti-α-tubulin (T9026, Sigma, 1:500). For IF analysis of testis tissues, freshly isolated testes were fixed in 4% paraformaldehyde (in PBS) and progressively embedded in optimal cutting temperature compound for frozen sectioning. Then, the cryosections were washed with PBS and blocked in 10% donkey serum containing 3% Triton X-100 before incubation with the following primary antibodies: rabbit polyclonal anti-SSX1 (PA5-61070, Invitrogen, 1:200) and anti-THY1 (LS-B3139, LSBio, 1:200). After the incubation of primary antibodies, both the sperm cell slides and testis cryosections were washed with PBS supplemented with 0.1% (v/v) Tween 20 and incubated with highly cross-adsorbed secondary antibodies Alexa Fluor 488 AffiniPure Donkey Anti-Mouse IgG (34106ES60, Yeasen, 1:1,000) and Cy3-conjugated AffiniPure Goat Anti-Rabbit IgG (111-165-003, Jackson, 1:4,000) for 1 h at room temperature. Images were acquired with a confocal microscope (Zeiss LSM 880).

RNA sequencing (RNA-seq)

For RNA-seq analysis, total RNA was extracted from the testicular tissues of tree shrews via the Allprep DNA/RNA/Protein Mini Kit (Qiagen) according to the manufacturer's protocol. RNA integrity was evaluated with 2100 Bioanalyzer (Agilent Technologies), and the RNA samples with an RNA integrity number ≥ 7 were used for library construction and subsequent sequencing analysis on the Illumina sequencing platform (NovaSeq 6000) by Oebiotech (Shanghai, China). Raw data (raw reads) were processed with Trimmomatic,[30] and reads containing poly-N and low-quality reads were removed. Then, the obtained clean reads were mapped to the tree shrew reference genome (TS_3.0, http://www.treeshrewdb.org/) with HISAT2.[31] For transcript-level quantification, the fragments per kilobase per million (FPKM)[31] and read count values of each protein-coding transcript were calculated by Bowtie2[32] and eXpress.[33] We identified differentially expressed genes (DEGs) by using the DESeq2[34] functions to estimate size factors and nbinom test. A fold change of >2 or <0.5 and $q < 0.05$ were set as the thresholds to identify significant differential expression. We performed hierarchical cluster analysis of DEGs to explore transcript expression patterns. Next, the DEGs were subjected to Gene Ontology enrichment and KEGG[35] pathway enrichment analyses by R based on the hypergeometric distribution. Networks were constructed by Cytoscape software (version 3.6.0).

Identification of testis-enriched genes in human and mouse

Published digital gene expression matrices (DGEs) for 27 different tissues from 95 human individuals were obtained from ArrayExpress (E-MTAB-1733). The DGEs of 70 mouse samples containing 13 different tissues were also downloaded from ArrayExpress (E-GEOD-43721, E-GEOD-74747, E-MTAB-2801, E-MTAB-4644, and E-MTAB-3718). Genes specifically or predominantly expressed in the testes of the two species were identified with the R package *DESeq2*[36] (FDR < 0.05; >2-fold higher normalized read counts in the testis compared with all other tissues). To define the orthologous genes that probably share conserved functions between human and mouse testes, we downloaded human-mouse one-to-one orthologs of acquired testis-enriched genes from the Ensembl database. For the identified orthologous pairs, only genes with specific or predominant expression patterns in the testis of both humans and mice were considered to have potentially similar testicular functions between the two species. Correspondingly, genes significantly enriched in the testis of one species but without a one-to-one ortholog or a similar testis-enriched expression pattern in the other species were considered to be genes specifically or predominantly expressed in the testis of only that species.

Results

Identification of deleterious variants of primate-specific *SSX1* in infertile men with asthenoteratozoospermia

To identify pathogenic genetic variants in asthenoteratozoospermia, we performed high-throughput WES on a cohort of 536 subjects affected by asthenoteratozoospermia (Figure 1A). After stringent bioinformatics analyses,[37] we identified six unrelated infertile men harboring hemizygous deleterious variants in *SSX1*, a PSG that has not been previously associated with any aspects of reproductive physiology in OMIM; these individuals accounted for 1.1% of our cohort. As summarized in Figure 1B, four individuals were found with hemizygous frameshift variants (N027 II-1: c.185_186del [p. Gly62Valfs*11]; H054 II-1: c.180del [p. Lys60Asnfs*2]; Y7460 II-1: c.351del [p. Glu118Argfs*58]; AY001 II-1: c.412_413del [p. Gln138Thrfs*11]) in *SSX1* (GenBank: NM_005635.3). All these variants introduce premature stop codons and are consequently expected to induce nonsense-mediated mRNA decay, which may affect protein synthesis. A hemizygous missense variant of *SSX1* (c.164A>G [p. Tyr55Cys]) was identified in the proband of family Y1642, and this variant was predicted by the PolyPhen-2, SIFT, CADD, and PROVEAN tools to be deleterious. Furthermore, we also identified a splice-site variant (c.*4+1G>A) of *SSX1* in subject S868 II-1. According to predictions from the Berkeley *Drosophila* Genome Project or Splice AI database and real-time qPCR analysis (Figure S3), the c.*4+1G>A variant abrogates the consensus donor site, leading to alternative splicing and significantly reduced expression of *SSX1*. All these six variants are absent or extremely rare in the human population genome datasets and predicted as pathogenic or likely pathogenic according to the guidelines from American College of Medical Genetics

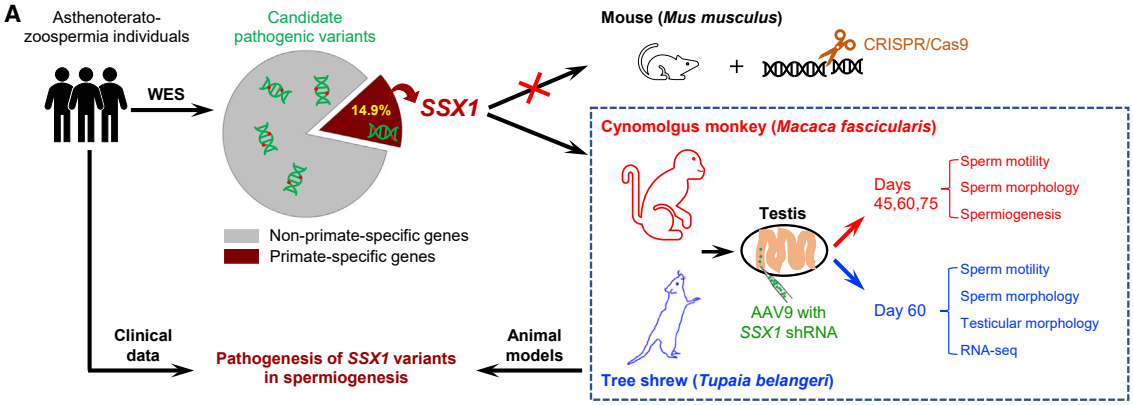

B Hemizygous deleterious *SSX1* variants identified in Chinese asthenoteratozoospermia-affected men

SSX1 variant (Individual)	V1 (N027 II-1)	V2 (H054 II-1)	V3 (Y1642 II-1)	V4 (Y7460 II-1)	V5 (AY001 II-1)	V6 (S868 II-1)
cDNA alteration	c.185_186del	c.180del	c.164A>G	c.351del	c.412_413del	c.*4+1G>A
Variant allele	hemizygous	hemizygous	hemizygous	hemizygous	hemizygous	hemizygous
Protein alteration	p.Gly62Valfs*11	p.Lys60Asnfs*2	p.Tyr55Cys	p.Glu118Argfs*58	p.Gln138Thrfs*11	–
Variant type	frameshift	frameshift	missense	frameshift	frameshift	splice-site
Allele frequency in human populations						
1000 Genomes Project	0	0	0	0	0	0
East Asians in gnomAD	0	0.0001622	0.0004265	0	0	0.0002696
All individuals in gnomAD	0	0.00001213	0.00006142	0	0	0.0001902
Function prediction						
SIFT	–	–	damaging	–	–	–
PolyPhen-2	–	–	damaging	–	–	–
PROVEAN	–	–	damaging	–	–	–
CADD	–	–	22.9	–	–	24.4
ACMG	pathogenic	pathogenic	likely pathogenic	pathogenic	pathogenic	pathogenic

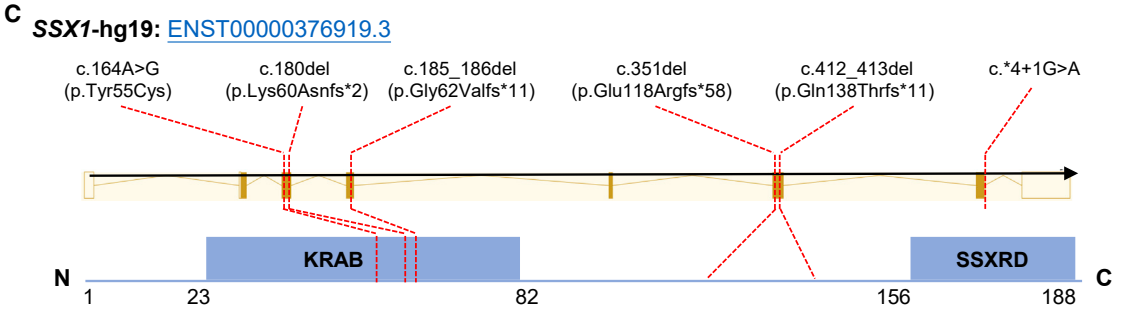

Figure 1. Identification and functional validation of hemizygous variants in X-linked *SSX1* in men with asthenoteratozoospermia
(A) Schematic illustration of the experimental design.
(B) Deleterious hemizygous *SSX1* variants identified in six unrelated infertile men affected by asthenoteratozoospermia. The NCBI reference sequence number of *SSX1* is GenBank: NM_005635.3. Variants with CADD values greater than 4 were considered to be deleterious. –, not applicable.
(C) Locations of the identified *SSX1* variants in relation to critical functional domains of SSX1. KRAB, Kruppel-associated box; SSXRD, SSX repression domain.

and Genomics. We performed Sanger sequencing to identify the existence of these variants, and the results are illustrated in Figure S4.

SSX1 (SSX family member 1; also known as cancer/testis antigen family 5, member 1) is located on the human chromosome X. SSX1 is specifically expressed in the testis and is mainly located in germ cells from spermatogonia to spermatocytes according to the Human Protein Atlas. In addition, SSX1 contains a Kruppel-associated box (KRAB) domain at the N terminus and an SSX repression domain (SSXRD) at the C terminus (Figure 1C), both of which are important for the function of SSX1 as a transcriptional repressor.[38] Notably, the *SSX1* variants identified in this study were predicted to affect the stability and function of SSX1. Further functional analyses by real-time qPCR and IF also indicated dramatic reduction in expressions of *SSX1* mRNA and protein in the spermatozoa of men harboring hemizygous *SSX1* variants (Figure S5). Therefore, all these

Table 1. Semen characteristics and sperm flagellar morphology in asthenoteratozoospermia-affected men harboring hemizygous *SSX1* variants

Individual	N027 II-1	H054 II-1	Y1642 II-1	Y7460 II-1	AY001 II-1	S868 II-1	Reference limits
Semen parameter							
Semen volume (mL)	4.0	3.4	2.5	3.1	2.2	4.8	1.5[a]
Sperm concentration (10^6/mL)	*9.5*	17.7	*11.6*	*4.9*	65.0	39.8	15.0[a]
Motility (%)	*0.0*	*33.8*	*0.0*	*24.0*	*2.0*	*27.2*	40.0[a]
Progressive motility (%)	*0.0*	*18.2*	*0.0*	*16.0*	*0.5*	*15.4*	32.0[a]
Sperm flagellar morphology							
Absent flagella (%)	*17.5*	–	*9.5*	*9.3*	2.7	2.0	5.0[b]
Short flagella (%)	*41.3*	–	*27.5*	*13.5*	*39.8*	*18.0*	1.0[b]
Coiled flagella (%)	*32.3*	–	*32.3*	*35.3*	*36.3*	*19.8*	17.0[b]
Angulation (%)	1.5	–	5.8	10.8	3.3	3.3	13.0[b]
Irregular caliber (%)	*4.0*	–	*9.3*	*22.0*	*7.0*	*6.3*	2.0[b]

The abnormal values are shown in italics.
–, not available.
[a]Reference limits according to the WHO standards.[26]
[b]Reference limits according to the distribution range of morphologically normal spermatozoa observed in 926 fertile individuals.[39]

findings suggested that *SSX1* is a PSG involved in human spermatogenesis.

SSX1 deficiency caused severe asthenoteratozoospermia phenotypes

Sperm analysis was carried out in source laboratories during routine biological examinations of the individuals according to the World Health Organization (WHO, 2010) guidelines.[26] All the men harboring hemizygous deleterious *SSX1* variants were shown to have severe-to-complete asthenoteratozoospermia phenotypes (Table 1). Sperm motility and progressive motility were dramatically decreased in these individuals with *SSX1* variants (Table 1). The morphology of the sperm cells was assessed by H&E staining and SEM. A variety of abnormal sperm morphologies were observed, including absent, short, coiled flagella and irregular caliber (Figure 2A). The rates of short and coiled flagella in the spermatozoa from men harboring hemizygous *SSX1* variants were significantly higher than those from normal reference values (Table 1).

We further conducted transmission electron microscopy (TEM) to investigate the ultrastructure of the sperm cells from individuals with *SSX1* variants. In comparison to the typical "9 + 2" axoneme microtubule structure in the sperm flagella from an unaffected individual, the spermatozoa from men harboring hemizygous *SSX1* variants displayed various ultrastructural defects, including the absence or misarrangement of outer dense fibers or microtubules at the midpiece and principal piece of sperm flagella (Figure 2B).

Asthenoteratozoospermia phenotypes were mimicked by KD of *Ssx1* expression in the testes of cynomolgus monkeys and tree shrews

To explore ideal animal models for investigating *SSX1*, phylogenetic analysis was performed on the basis of protein sequences of SSX family members from mice, tree shrews, cynomolgus monkeys, and humans. As shown in Figure S6, human SSX1 has closer evolutionary distances with cynomolgus monkey SSX1 and tree shrew SSX1 than those of mouse SSX family members. To further investigate the role of primate-specific *SSX1* in spermatogenesis, we developed an *in vivo* KD system based on the microinjection of *Ssx1*-shRNA-containing, enhanced green fluorescent protein (EGFP)-expressing AAV9 vectors into the seminiferous tubules of the testes of adult male cynomolgus monkeys through the rete testis under ultrasound guidance. Semen samples and testicular biopsy samples were collected before injection and 45, 60, and 75 days after injection. To confirm the KD efficacy of monkey *Ssx1 in vivo*, we performed a real-time qPCR assay by using testicular biopsy samples, and we observed a dramatically reduced abundance of *Ssx1* mRNA in the *Ssx1*-KD group (Figure S7). H&E staining of testicular sections from the *Ssx1*-KD male cynomolgus monkeys indicated abnormal spermatogenesis, as shown by abnormal arrangements of germ cells (Figure 3A). Sperm morphology was also analyzed with SEM. Similar to what was observed in men harboring hemizygous *SSX1* variants, a higher rate of absent, short, or coiled flagella was observed in the sperm cells from the *Ssx1*-KD group than that in the NC group (Figure 3B). In addition, TEM observations on spermatozoa from the *Ssx1*-KD male cynomolgus monkeys also revealed a lack of microtubules or a disorganization of outer dense fibers (Figure 3C). Sperm motility was significantly reduced in the *Ssx1*-KD group (Figure 3D). Notably, the reduced sperm motility and abnormal sperm morphology were obvious at 45 days after injection but almost recovered at 75 days after injection (Figure 3D).

Tree shrews, close relatives of primates, have the advantageous features of small adult body size, short reproductive cycle and life span, and low cost of maintenance[40];

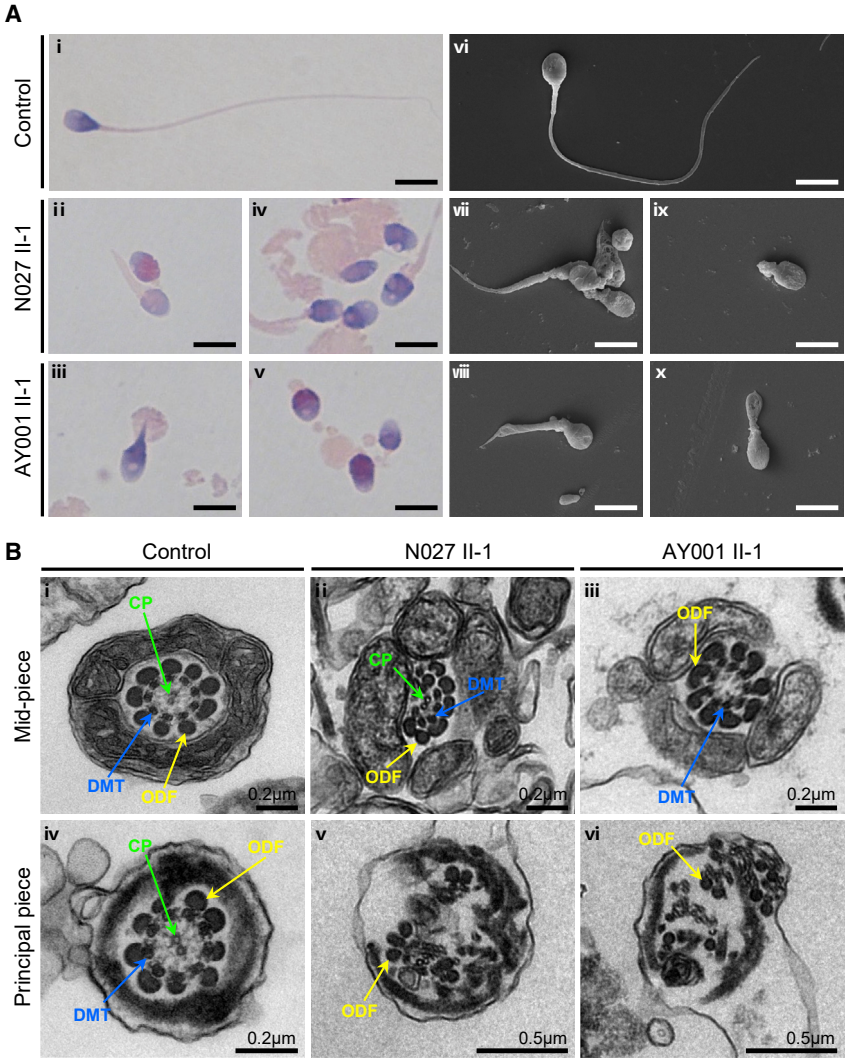

Figure 2. Morphology and ultrastructure analyses of sperm from men harboring hemizygous *SSX1* variants

(A) Morphology analyses of spermatozoa by H&E staining (i–v) and SEM (vi–x). Normal morphology was observed in the spermatozoon from a healthy control male (i and vi). Most spermatozoa from *SSX1*-deficient men had flagella that were absent (v and ix), short (iv, vii, and viii), coiled (iii and x), or of irregular caliber (iv and v). Scale bars: 5 μm.

(B) TEM analysis of the spermatozoa from a control male individual and men harboring hemizygous *SSX1* variants. In the cross-sections of the spermatozoa from a fertile control subject, the typical "9 + 2" microtubule structures were clearly observed (i and iv). Cross-sections of the spermatozoa from men harboring hemizygous *SSX1* variants displayed various ultrastructural abnormalities in sperm flagella, including misarranged ODFs (v and vi) and missing DMTs and/or the CP (ii, iii, v, and vi). Abbreviations: CP, central pair of microtubules (green arrows); DMT, peripheral microtubule doublet (blue arrows); ODF, outer dense fiber (yellow arrows).

therefore, tree shrews have been used as a viable alternative animal model to primates in biomedical research.[14,41] *Ssx1* is also predominantly expressed in the testis of tree shrew according to the Tree shrew database.[17] To further confirm the asthenoteratozoospermia phenotypes observed in *Ssx1*-KD male cynomolgus monkeys, we also constructed an *in vivo Ssx1*-KD model in tree shrews. *Ssx1*-shRNA-containing and EGFP-expressing AAV9 vectors were injected into seminiferous tubules via the rete testis. Semen samples and testis tissues were collected at 60 days (after a complete spermatogenic cycle) after injection. As shown in Figure 4A, green seminiferous tubules were clearly visible on the 60th day after injection with the AAV9 vectors. IF staining of testicular tissue sections with an antibody against THY1, which is a marker of spermatogonia, indicated that the AAV9 vectors reached and infected the spermatogonia (Figure 4B). Real-time qPCR assay suggested that the abundance of *Ssx1* mRNA was significantly reduced in the testes of the *Ssx1*-KD group (Figure S8A). Consistently, immunoblotting and immunostaining assays also revealed a dramatically reduced accumulation of SSX1 in the testes of the *Ssx1*-KD group (Figures S8B and S8C). Testis weight was significantly reduced in the *Ssx1*-KD group when compared to the NC group (Figure S9). H&E staining of testis sections from the *Ssx1*-KD male tree shrews revealed abnormal spermatogenesis, including impaired spermatogenesis or the loss of germ cells from seminiferous tubules (Figure S10). H&E staining also revealed various abnormal sperm morphologies, including absent, coiled, or angulated flagella (Figure 4C). Furthermore, TEM observations on the sperm ultrastructure of the *Ssx1*-KD male tree shrews revealed the absence of peripheral or central microtubules at the midpiece and principal piece of sperm flagella (Figure 4D). Semen characteristics were investigated by a computer-assisted sperm analysis (CASA) system, and significant decreases in sperm motility and progressive motility were observed in the *Ssx1*-KD group (Figures 5A and 5B). Regarding sperm locomotion parameters, the curvilinear velocity (VCL), straight-line velocity (VSL), average-path velocity (VAP), amplitude of lateral head displacement (ALH), and beat cross frequency (BCF) were significantly lower in the *Ssx1*-KD group than those in the NC group (Figure 5C).

Abnormal expressions of multiple spermatogenesis-associated factors in the *Ssx1*-KD model

High-throughput RNA-seq was performed with the testicular tissues from *Ssx1*-KD and NC male tree shrews. A total of 658 genes (484 up-regulated and 174 down-regulated) were differentially expressed (fold-change > 2 or < 0.5 and $q < 0.05$) in the *Ssx1*-KD testes compared to the NC testes (Figure 6A). Gene Ontology analysis indicated that these

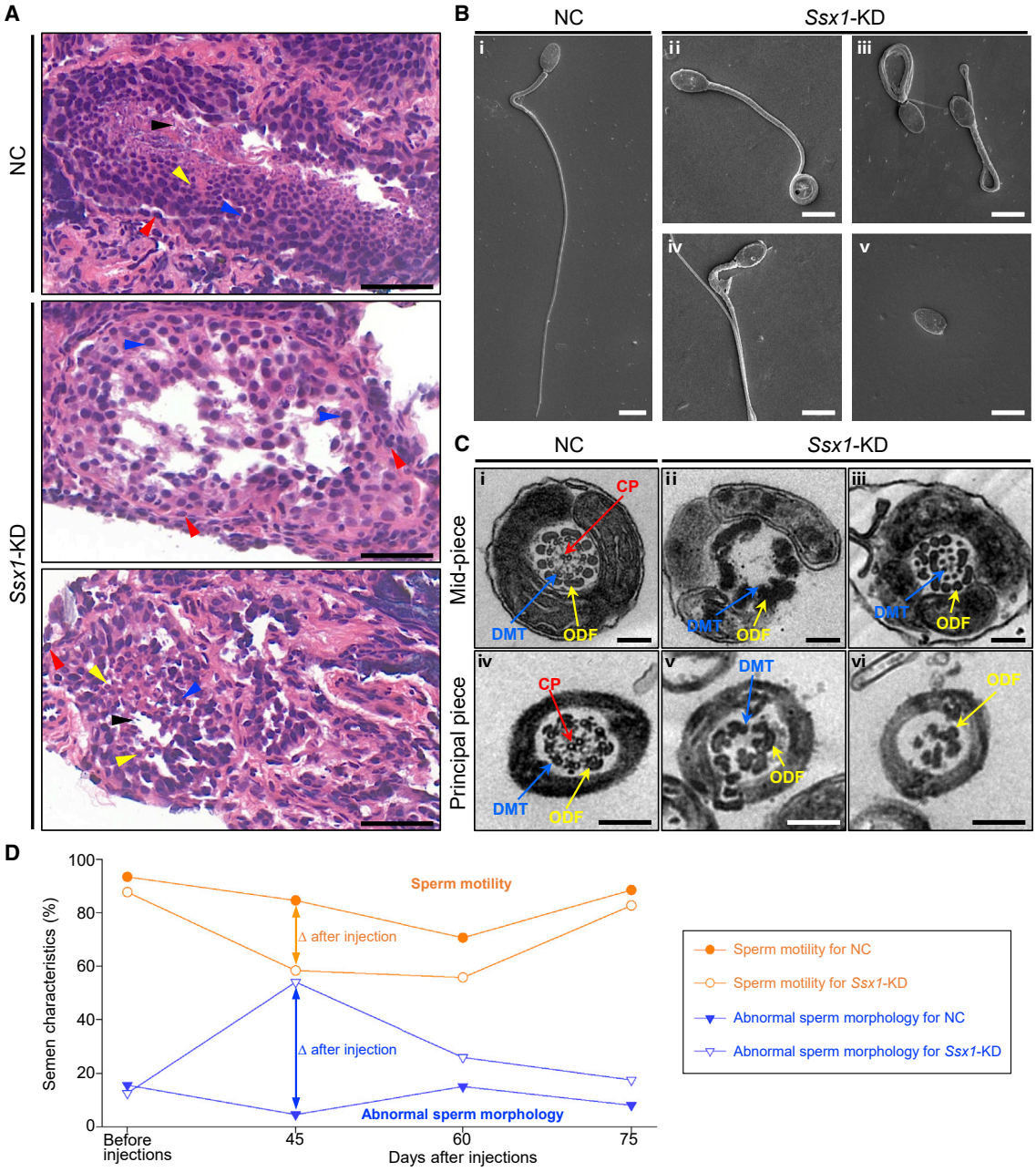

Figure 3. Cynomolgus monkey model revealed defective spermatogenesis and abnormal sperm morphologies in the *Ssx1*-KD testes

(A) H&E staining of testicular tissue sections obtained from male cynomolgus monkeys. Compared to the regular arrangement of various germ cells in the testes from the NC group, spermatogenic defects, including loss or misarranged germ cells, were observed in the testes from *Ssx1*-KD male cynomolgus monkeys; spermatogonia (red arrowheads), spermatocytes (blue arrowheads), round spermatids (yellow arrowheads), and spermatozoa (black arrowheads). Scale bars: 50 μm.

(B) Abnormal morphologies were also observed in the sperm from *Ssx1*-KD male cynomolgus monkeys, including coiled (ii, iii), bending (iv), and absent (v) flagella. Scale bars: 5 μm.

(C) Compared to the typical "9 + 2" microtubule structures in the sperm flagella of the NC group (i and iv), *Ssx1*-KD in the testes also led to various ultrastructural abnormalities in the sperm flagella, including the misarranged or missing ODFs (iii, v, and vi) and the loss of DMTs or CP (ii, iii, v, and vi). Scale bars: 200 nm. Abbreviations: CP, central pair of microtubules (red arrows); DMT, peripheral microtubule doublet (blue arrows); ODF, outer dense fiber (yellow arrows).

(D) *Ssx1*-KD in the testes of male cynomolgus monkeys led to temporary abnormalities in sperm motility and morphology after injections. The values for the NC group represent three repeated statistical analyses of one cynomolgus monkey, and the values for *Ssx1*-KD group represent the mean data from three male cynomolgus monkeys. For each cynomolgus monkey, at least 200 spermatozoa were examined to evaluate the rates of morphologically abnormal spermatozoa.

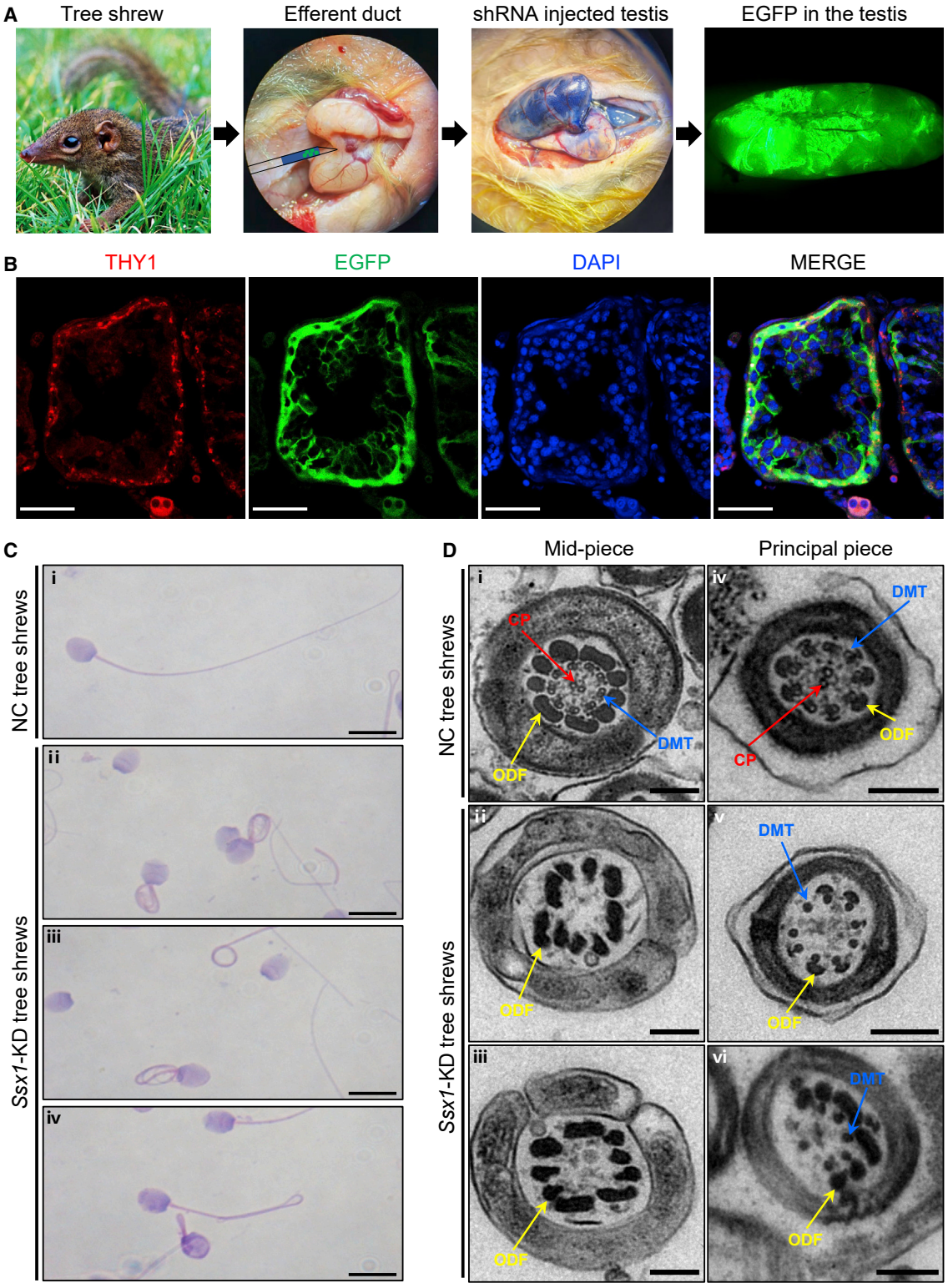

Figure 4. Injections of AAV9-*Ssx1*-shRNA vectors into the testes of male tree shrews and sperm morphological abnormalities in the *Ssx1*-KD group

(A) AAV9-*Ssx1*-shRNA vectors or AAV9-NC-shRNA vectors were injected into the seminiferous tubules of tree shrew testes through the rete testis, and Trypan blue was used as a tracer. The signal of enhanced green fluorescent protein (EGFP) expressed by AAV9-*Ssx1*-shRNA vectors also indicated effective infection of the AAV9-*Ssx1*-shRNA vectors into the seminiferous tubules.

(B) IF staining of THY1 (a marker of spermatogonia) in testicular tissue sections after injections of AAV9-*Ssx1*-shRNA vectors or AAV9-NC-shRNA vectors. The colocalization of THY1 and EGFP indicated that the injected AAV9 penetrated the BTB and reached the spermatogonia. DNA was counterstained with DAPI (4′,6-diamidino-2-phenylindole) as a marker of cell nuclei. Scale bars: 50 μm.

(legend continued on next page)

transcriptionally dysregulated genes were significantly enriched in multiple biological processes or components associated with cytogenesis or transcription regulation, the details are shown in Figure 6B. Notably, the downregulated genes included various genes required for spermatogenesis and ciliogenesis, including eight genes involved in "microtubule" (*Cep170*, *Dnm3*, *Eml5*, *Golga2li6*, *Golga2li9*, *Kif21b*, *Ttll7*, and *Ttll10*), four genes involved in "spermatid development" (*Cdyl*, *Dpy19l2*, *Fndc3a*, and *Ica1l*), seven genes involved in "cilium" (*Alms1*, *Cfap58*, *Fank1*, *Iqce*, *Kifap3*, *Ttll7*, and *Ttll10*), nine genes involved in "centrosome" (*Alms1*, *C2cd3*, *Ccdc81*, *Cep44*, *Cep164*, *Cep170*, *Kifap3*, *Lrrcc1*, and *Rapgef6*), six genes involved in "cell division" (*Cep164*, *Cuzd1*, *Evi5*, *Lrrcc1*, *Mad1l1*, and *Tent4b*), four genes involved in "axoneme" (*Ccdc39*, *Kifap3*, *Ttll10*, and *Wdpcp*), three genes involved in "ciliary basal body-plasma membrane docking" (*Alms1*, *C2cd3*, and *Cep164*), three genes involved in "protein deubiquitination" (*Smurf2*, *Usp1*, and *Usp47*), and six genes involved in mRNA catabolic process, mRNA export, or transcription initiation (*Cmtr2*, *Gtf2a1L*, *Nr4a2*, *Taf5*, *Upf1*, and *Upf2*) (Figure 6C). We performed real-time qPCR to further verify the significantly decreased expression of these genes (Figure 6D). In addition, Western blotting assay also confirmed the decreased protein levels of multiple selected candidates (Figure S11). Taken together, these findings indicate that *Ssx1* deficiency may influence multiple biological processes involved in spermatogenesis.

Damaged male fertility resulting from *SSX1* deficiency may be rescued by intra-cytoplasmic sperm injection (ICSI) treatment

ICSI treatment has been suggested as a common clinical therapeutic strategy to circumvent the infertility associated with asthenoteratozoospermia. In this study, five of the six men harboring hemizygous *SSX1* variants received assisted reproductive therapy via ICSI. As shown in Table 2, three (H054 II-1, Y7460 II-1, and AY001 II-1) of the five couples achieved a successful pregnancy. For the other two couples (N027 II-1 and S868 II-1), 8-cell embryos or blastocysts were developed and used for embryo transfer while no good ICSI outcome was achieved, which could be partially attributed to older age (e.g., couple S868 II-1), poor quality of the oocytes from the female partners, or other reasons. Overall, ICSI treatment is favorable for the *SSX1*-associated asthenoteratozoospermia.

Discussion

As new genes that contribute to phenotypic evolution, PSGs, especially X-linked PSGs, are often predominantly or specifically transcribed in the testis.[42,43] Among the newly identified PSGs in the human genome, more than 30% of genes are testis enriched.[10] Consistently, PSG variants account for 14.9% of all the candidate pathogenic variants identified in the infertile individuals of this study (Figure 1A). Furthermore, we conducted differential expression analysis by using transcriptional data from the Expression Atlas database and revealed 1,477 human testis-enriched genes that lack one-to-one orthologs in mice or whose murine orthologs do not exhibit a significantly testis-enriched expression pattern; these human genes account for 49.7% of all human genes that are specifically or predominantly expressed in the testis (Figure S12). All these findings identified high rates of PSG expressions in the testis, but limited studies have revealed their functions in spermatogenesis.

In the present work, our genetic analyses using WES identified six unrelated infertile men with asthenoteratozoospermia who carried hemizygous variants in *SSX1*; this gene is PSG preferentially expressed in the testis. Notably, all these *SSX1* variants are either rare or absent from human population genome datasets and are predicted to be deleterious variants according to multiple bioinformatic tools. Further analyses indicated that the expression of *SSX1* was significantly reduced in the spermatozoa from men harboring hemizygous *SSX1* variants. Therefore, all these findings indicate that the phenotypes associated with asthenoteratozoospermia in these individuals are likely to be explained by the hemizygous deleterious variants in primate-specific *SSX1*.

For studies about PSGs, mouse model is not applicable. To explore the effect of *SSX1* deficiency on spermatogenesis, we constructed two *Ssx1*-KD models by injecting AAV9-*Ssx1*-shRNA vectors into the seminiferous tubules of the testes of adult male cynomolgus monkeys and tree shrews. Colocalization of green fluorescent protein expressed by AAV9 vectors and THY1 (a marker of spermatogonia) indicated that the AAV9-*Ssx1*-shRNA vectors penetrated the BTB, reaching and infecting the spermatogonia. Further functional analyses revealed significantly reduced expression of *Ssx1* in the testes of *Ssx1*-KD male cynomolgus monkeys and tree shrews, indicating the successful establishment of the *in vivo* *Ssx1*-KD models. Notably, both *Ssx1*-KD models displayed reduced sperm motility and abnormal sperm morphology, which was consistent with the clinical presentation of men harboring hemizygous deleterious variants in *SSX1*, further confirming the important role of *SSX1* in normal spermatogenesis. In particular, the *Ssx1*-KD male cynomolgus monkeys displayed obviously reduced sperm motility and abnormal

(C) H&E staining of spermatozoa from NC and *Ssx1*-KD male tree shrews. Abnormal sperm morphologies, including absent, short, coiled, or bending flagella, were detected in sperm samples from *Ssx1*-KD male tree shrews. Scale bars: 20 μm.
(D) TEM analysis of spermatozoa from NC and *Ssx1*-KD male tree shrews. Consistent with those observed in *SSX1*-deficient men and *Ssx1*-KD male cynomolgus monkeys, the ultrastructures of the spermatozoa from *Ssx1*-KD male tree shrews also displayed misarrangements or loss of DMTs or CP (ii, iii, v, vi). Scale bars: 200 nm. Abbreviations: CP, central pair of microtubules (red arrows); DMT, peripheral microtubule doublet (blue arrows); ODF, outer dense fiber (yellow arrows).

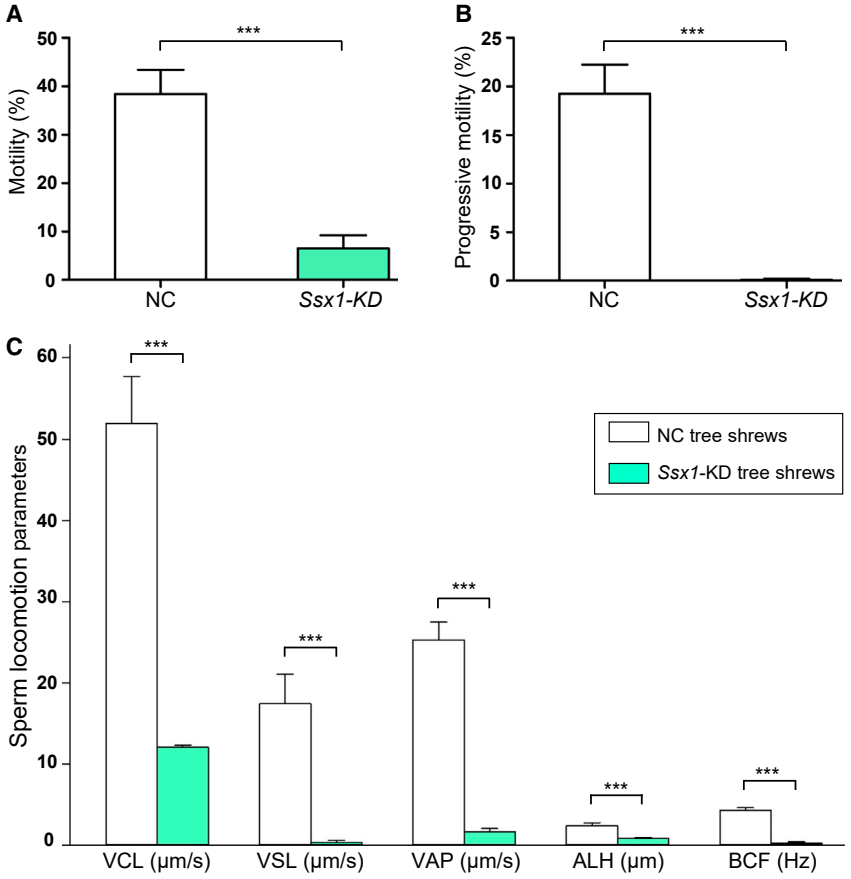

Figure 5. Semen characteristics of *Ssx1*-KD male tree shrews

(A–C) Semen characteristics assessed by a CASA system revealed significant reductions in sperm motility (A) and progressive motility (B) in *Ssx1*-KD male tree shrews when compared with those from NC male tree shrews. The curvilinear velocity (VCL), straight-line velocity (VSL), average-path velocity (VAP), amplitude of lateral head displacement (ALH), and beat cross frequency (BCF) were also dramatically decreased in the *Ssx1*-KD group (C). For each group, at least five tree shrews were analyzed. The error bars represent the SEM. ***$p < 0.001$.

sperm morphologies at 45 days after injection, but this phenotypic abnormality was almost recovered at 75 days after injection. This indicated the flexibility of the AAV-mediated KD system and suggested the possibility of using synthetic biological sequences for highly specific male contraceptives.

As described above, the asthenoteratozoospermia phenotypes associated with *SSX1* deficiency were reproduced in *Ssx1*-KD male cynomolgus monkeys and tree shrews, indicating that AAV9 combined with shRNA-mediated gene expression KD could be a tool for *in vivo* genetic manipulation of male reproductive systems (especially for the manipulation of genes that are not present in mice or that are evolutionarily differentiated in function). As two model organisms that are close relatives to humans, cynomolgus monkeys and tree shrews had different advantages for research on reproductive diseases via the AAV-shRNA-mediated gene KD system. The cynomolgus monkey model can be used to mimic the steps of semen collection in human, which was convenient for semen parameter analyses at different time points after the gene KD. Moreover, short-term *in vivo* genetic intervention in adult monkeys significantly shortened the period required for observations on reproductive phenotypes when compared to the previous strategy for germline gene editing; in the latter case, at least 4–5 years are needed for acquiring gene edited offspring and the subsequent appearance of reproductive phenotyping in adults. Furthermore, the efficacy to generate gene-edited monkeys is extremely low so far. Thus, our findings indicated that the monkey model and the AAV-shRNA-mediated gene KD system are suitable for phenotypic analysis and mechanistic studies on human reproductive disorders of genetic origin. For tree shrews, their small adult body size and short reproductive cycle make them easy to collect sperm samples or testis tissues for phenotypic and mechanistic studies. Because of their close proximity to primates, tree shrews with AAV-shRNA-mediated gene expression KD are also ideal models for exploring the molecular mechanisms underlying diseases caused by abnormal gene expressions in human. Therefore, our study, which was based on AAV-shRNA-mediated gene expression KD in two model organisms, provides two experimental systems for research with different purposes.

To gain insights into the molecular mechanisms underlying *SSX1*-associated asthenoteratozoospermia, we performed high-throughput RNA-seq by using the testicular tissues from *Ssx1*-KD and NC male tree shrews. Notably, DEGs were enriched in multiple biological processes involved in spermatogenesis, including protein deubiquitination, transcription initiation, and mRNA catabolic processes. For example, *C2cd3*, which encodes a positive regulator of centriole elongation,[44] was found to be expressed at significantly decreased levels in the testes of *Ssx1*-KD male tree shrews. Furthermore, we also detected a lower abundance of *Fndc3a*, which encodes a protein required for adhesion between spermatids and Sertoli cells,[45] in the *Ssx1*-KD group than in the NC group. In addition, significantly reduced expressions of two RNA surveillance proteins,[46] UPF1 and UPF2, were also observed in the *Ssx1*-KD group. A previous study reported that the disruption of *Upf2* during the early stages of spermatogenesis resulted in the disappearance of nearly all

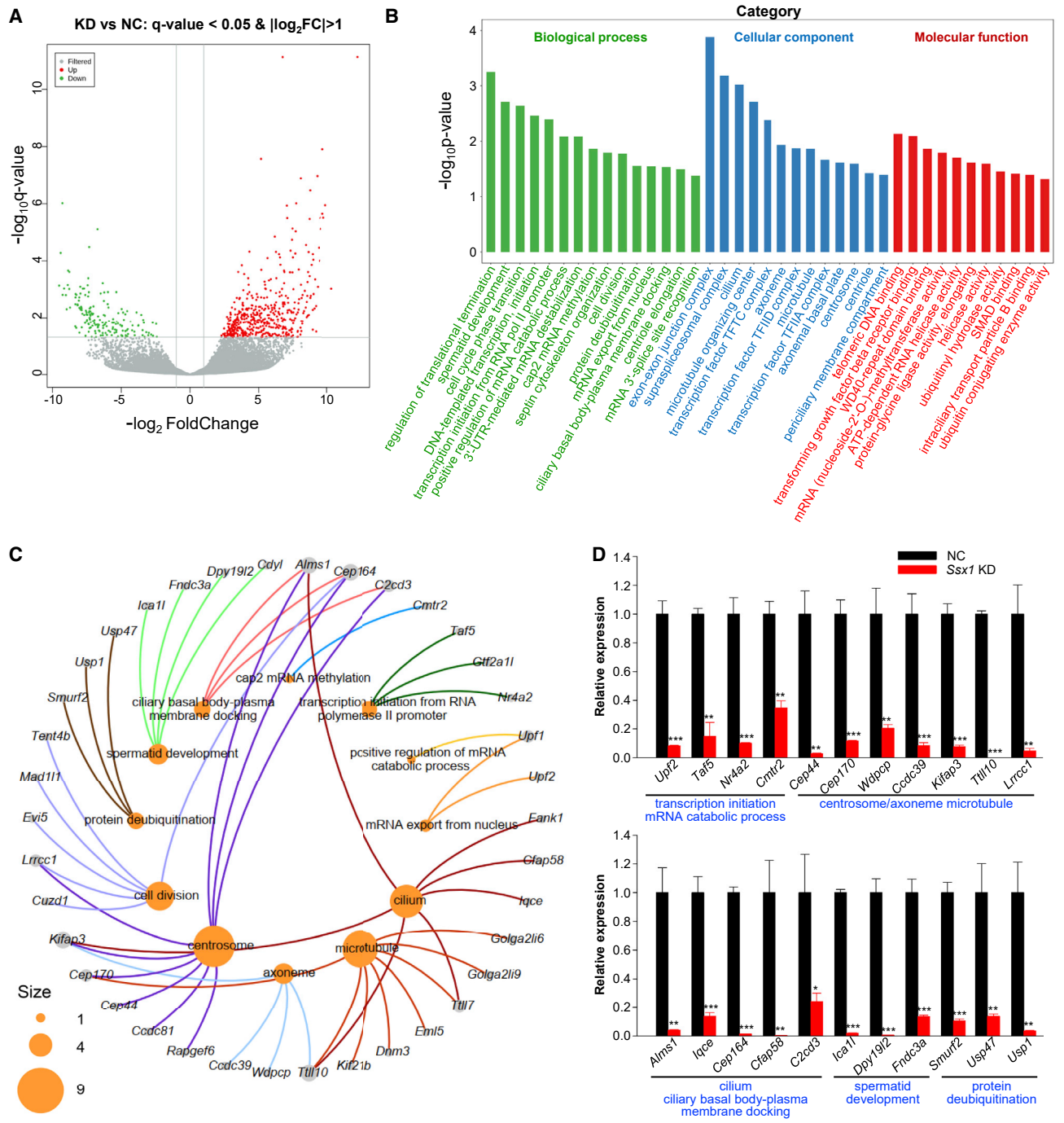

Figure 6. ***Ssx1*-KD in the testis alters the expression pattern of genes involved in spermatogenesis**

(A) Volcano plot showing the DEGs between NC and *Ssx1*-KD testes of male tree shrews. A 2-fold difference in expression and q = 0.05 were used as the cutoff.

(B) Gene Ontology (GO) analysis of transcriptionally dysregulated genes.

(C) Network diagram of gene-GO terms revealed that the downregulated genes included various genes required for spermatogenesis or ciliogenesis. The size of the circles represents the number of genes enriched in a particular GO term.

(D) Real-time qPCR validation of a portion of downregulated genes in the testes of *Ssx1*-KD male tree shrews. The data are presented as the mean ± SE of three independent experiments. Two-tailed Student's paired or unpaired t tests were used as appropriate (*$p < 0.05$; **$p < 0.01$; ***$p < 0.001$).

spermatogenic cells through the loss of nonsense-mediated mRNA decay.[47] Therefore, all these findings may partially explain the abnormal spermatogenesis observed in the *Ssx1*-KD group.

ICSI, which is a kind of assisted reproduction technique, has been an effective method for treating male infertility caused by asthenoteratozoospermia because it overcomes the fertilization failure caused by decreased sperm vitality

Table 2. Clinical outcomes of ICSI cycles with spermatozoa from men harboring hemizygous *SSX1* variants

Individual	N027 II-1	H054 II-1	Y1642 II-1	Y7460 II-1	AY001 II-1	S868 II-1
Male age (years)	29	26	22	32	31	31
Female age (years)	25	28	21	32	29	35
Number of ICSI cycle	1	1	–	1	1	1
Number of oocytes injected	5	15	–	14	28	15
Number (and rate) of fertilized oocytes	5 (100.0%)	14 (93.0%)	–	12 (86.0%)	27 (96.4%)	14 (93.3%)
Number (and rate) of cleavage embryos	5 (100.0%)	14 (100.0%)	–	12 (100.0%)	26 (96.3%)	14 (100.0%)
Number (and rate) of 8-cells	4 (80.0%)	11 (78.6%)	–	10 (83.3%)	20 (74.1%)	12 (85.7%)
Number (and rate) of blastocysts	–	8 (57.1%)	–	10 (83.3%)	12 (44.4%)	9 (64.3%)
Number of transfer cycle(s)	1	1	–	1	1	2
Number of embryo(s) transferred per cycle	2	2	–	2	1	1
Implantation rate	0.0%	100.0%	–	50.0%	100.0%	0.0%
Clinical pregnancy rate	0.0%	100.0%	–	100.0%	100.0%	0.0%
Miscarriage rate	–	0.0%	–	0.0%	0.0%	–

–, not applicable.

or abnormal sperm morphologies. Previous studies and our recent studies have also revealed good prognosis of ICSI treatment for a series of asthenoteratozoospermia-related genes, including *DNAH1*, *DNAH8*, *CFAP47*, and *TTC29*.[19,37,48,49] In this study, five of the six men harboring hemizygous *SSX1* variants received ICSI treatment with their own sperm, and three of the five couples achieved a successful pregnancy. For the other two couples (N027 II-1 and S868 II-1), 8-cell embryos or blastocysts were also developed. Therefore, ICSI treatment is promising and can also be recommended for the individuals with *SSX1*-associated asthenoteratozoospermia.

In summary, our study identified primate-specific *SSX1* as a genetic factor for human male infertility with asthenoteratozoospermia. ICSI treatment is favorable for the *SSX1*-associated asthenoteratozoospermia. In addition to the PSG *SSX1*, a high proportion of genes whose expression is testis-enriched but are not evolutionarily conserved between humans and mice were also identified. Specifically, this study established the AAV9-shRNA-mediated gene expression KD system based on the cynomolgus monkey and tree shrew models, which provide a promising strategy for *in vivo* spermatogenic studies of essential factors that cannot be achieved via the murine models. Overall, combining clinical studies, human genetics, *in vivo* genetic manipulation, and high-resolution transcriptome analysis, this study provides an approach that might help to further understand the genetic causes of male infertility and develop contraception or personalized therapies for reproductive defects.

Supplemental information

Supplemental information can be found online at https://doi.org/10.1016/j.ajhg.2023.01.016.

Acknowledgments

We would like to thank the families for participating and supporting this study and the Center of Cryo-electron Microscopy at Zhejiang University for technical support. This study was supported by the National Key Research and Development Program of China (2021YFC2701400, 2018YFA0801400, 2018YFC1004901, and 2021YFC2700901), the National Natural Science Foundation of China (32288101, 32100480, 81971447, 82171608, 82101961, 81971441, and 82171607), the Scientific Research (TP202002) from Anhui Medical University, the China Postdoctoral Science Foundation (2020TQ0072), Yunnan Major Scientific and Technological Project (202202AG050018), the Chinese Academy of Sciences (Light of West China Program xbzg-zdsys-201909), and the Key Grant of Prevention and Treatment of Birth Defect from Hunan Province (2019SK1012).

Declaration of interests

The authors declare no competing interests.

Received: September 21, 2022
Accepted: January 19, 2023
Published: February 15, 2023

Web resources

1000 Genomes Project, http://www.internationalgenome.org
Berkeley *Drosophila* Genome Project, https://www.fruitfly.org/
CADD, https://cadd.gs.washington.edu/snv
Ensembl, http://www.ensembl.org/index.html
Expression Atlas, https://www.ebi.ac.uk/gxa/home
gnomAD, https://gnomad.broadinstitute.org
Human Protein Atlas, https://www.proteinatlas.org
National Center for Biotechnology Information (NCBI), https://www.ncbi.nlm.nih.gov/
NNSPLICE 0.9, http://www.fruitfly.org/seq_tools/splice.html
OMIM, http://www.omim.org/

Picard, https://github.com/broadinstitute/picard
PolyPhen-2, http://genetics.bwh.harvard.edu/pph2/
PROVEAN, https://www.jcvi.org/research/provean
SIFT, https://sift.bii.a-star.edu.sg
SpliceAI, https://spliceailookup.broadinstitute.org/
Tree shrew Database, http://www.treeshrewdb.org/
UCSC Genome Browser, http://genome.ucsc.edu

References

1. Inhorn, M.C., and Patrizio, P. (2015). Infertility around the globe: new thinking on gender, reproductive technologies and global movements in the 21st century. Hum. Reprod. Update *21*, 411–426.
2. Cavallini, G. (2006). Male idiopathic oligoasthenoteratozoospermia. Asian J. Androl. *8*, 143–157.
3. Touré, A., Martinez, G., Kherraf, Z.E., Cazin, C., Beurois, J., Arnoult, C., Ray, P.F., and Coutton, C. (2021). The genetic architecture of morphological abnormalities of the sperm tail. Hum. Genet. *140*, 21–42.
4. Ben Khelifa, M., Coutton, C., Zouari, R., Karaouzène, T., Rendu, J., Bidart, M., Yassine, S., Pierre, V., Delaroche, J., Hennebicq, S., et al. (2014). Mutations in DNAH1, which encodes an inner arm heavy chain dynein, lead to male infertility from multiple morphological abnormalities of the sperm flagella. Am. J. Hum. Genet. *94*, 95–104.
5. Tang, S., Wang, X., Li, W., Yang, X., Li, Z., Liu, W., Li, C., Zhu, Z., Wang, L., Wang, J., et al. (2017). Biallelic Mutations in CFAP43 and CFAP44 cause male infertility with multiple morphological abnormalities of the sperm flagella. Am. J. Hum. Genet. *100*, 854–864.
6. Kherraf, Z.E., Conne, B., Amiri-Yekta, A., Kent, M.C., Coutton, C., Escoffier, J., Nef, S., Arnoult, C., and Ray, P.F. (2018). Creation of knock out and knock in mice by CRISPR/Cas9 to validate candidate genes for human male infertility, interest, difficulties and feasibility. Mol. Cell. Endocrinol. *468*, 70–80.
7. Young, S.A.M., Aitken, R.J., and Ikawa, M. (2015). Advantages of using the CRISPR/Cas9 system of genome editing to investigate male reproductive mechanisms using mouse models. Asian J. Androl. *17*, 623–627.
8. Kiyozumi, D., Noda, T., Yamaguchi, R., Tobita, T., Matsumura, T., Shimada, K., Kodani, M., Kohda, T., Fujihara, Y., Ozawa, M., et al. (2020). NELL2-mediated lumicrine signaling through OVCH2 is required for male fertility. Science *368*, 1132–1135.
9. Yuan, S., Liu, Y., Peng, H., Tang, C., Hennig, G.W., Wang, Z., Wang, L., Yu, T., Klukovich, R., Zhang, Y., et al. (2019). Motile cilia of the male reproductive system require miR-34/miR-449 for development and function to generate luminal turbulence. Proc. Natl. Acad. Sci. USA *116*, 3584–3593.
10. Shao, Y., Chen, C., Shen, H., He, B.Z., Yu, D., Jiang, S., Zhao, S., Gao, Z., Zhu, Z., Chen, X., et al. (2019). GenTree, an integrated resource for analyzing the evolution and function of primate-specific coding genes. Genome Res. *29*, 682–696.
11. Mueller, J.L., Skaletsky, H., Brown, L.G., Zaghlul, S., Rock, S., Graves, T., Auger, K., Warren, W.C., Wilson, R.K., and Page, D.C. (2013). Independent specialization of the human and mouse X chromosomes for the male germ line. Nat. Genet. *45*, 1083–1087.
12. Vockel, M., Riera-Escamilla, A., Tüttelmann, F., and Krausz, C. (2021). The X chromosome and male infertility. Hum. Genet. *140*, 203–215.
13. Chen, Y., Niu, Y., and Ji, W. (2012). Transgenic nonhuman primate models for human diseases: approaches and contributing factors. J. Genet. Genom. *39*, 247–251.
14. Fan, Y., Huang, Z.Y., Cao, C.C., Chen, C.S., Chen, Y.X., Fan, D.D., He, J., Hou, H.L., Hu, L., Hu, X.T., et al. (2013). Genome of the Chinese tree shrew. Nat. Commun. *4*, 1426.
15. Rockland, K.S., and Lund, J.S. (1982). Widespread periodic intrinsic connections in the tree shrew visual cortex. Science *215*, 1532–1534.
16. Fan, Y., Ye, M.S., Zhang, J.Y., Xu, L., Yu, D.D., Gu, T.L., Yao, Y.L., Chen, J.Q., Lv, L.B., Zheng, P., et al. (2019). Chromosomal level assembly and population sequencing of the Chinese tree shrew genome. Zool. Res. *40*, 506–521.
17. Fan, Y., Yu, D., and Yao, Y.G. (2014). Tree shrew database (TreeshrewDB): a genomic knowledge base for the Chinese tree shrew. Sci. Rep. *4*, 7145.
18. Ye, M.S., Zhang, J.Y., Yu, D.D., Xu, M., Xu, L., Lv, L.B., Zhu, Q.Y., Fan, Y., and Yao, Y.G. (2021). Comprehensive annotation of the Chinese tree shrew genome by large-scale RNA sequencing and long-read isoform sequencing. Zool. Res. *42*, 692–709.
19. Liu, C., Tu, C., Wang, L., Wu, H., Houston, B.J., Mastrorosa, F.K., Zhang, W., Shen, Y., Wang, J., Tian, S., et al. (2021). Deleterious variants in X-linked CFAP47 induce asthenoteratozoospermia and primary male infertility. Am. J. Hum. Genet. *108*, 309–323.
20. Li, H., and Durbin, R. (2010). Fast and accurate long-read alignment with Burrows-Wheeler transform. Bioinformatics *26*, 589–595.
21. Wang, K., Li, M., and Hakonarson, H. (2010). ANNOVAR: functional annotation of genetic variants from high-throughput sequencing data. Nucleic Acids Res. *38*, e164.
22. Ashburner, M., Ball, C.A., Blake, J.A., Botstein, D., Butler, H., Cherry, J.M., Davis, A.P., Dolinski, K., Dwight, S.S., Eppig, J.T., et al. (2000). Gene Ontology: tool for the unification of biology. Nat. Genet. *25*, 25–29.
23. Kumar, P., Henikoff, S., and Ng, P.C. (2009). Predicting the effects of coding non-synonymous variants on protein function using the SIFT algorithm. Nat. Protoc. *4*, 1073–1081.
24. Adzhubei, I.A., Schmidt, S., Peshkin, L., Ramensky, V.E., Gerasimova, A., Bork, P., Kondrashov, A.S., and Sunyaev, S.R. (2010). A method and server for predicting damaging missense mutations. Nat. Methods *7*, 248–249.
25. Schwarz, J.M., Cooper, D.N., Schuelke, M., and Seelow, D. (2014). MutationTaster2: mutation prediction for the deep-sequencing age. Nat. Methods *11*, 361–362.
26. Cooper, T.G., Noonan, E., von Eckardstein, S., Auger, J., Baker, H.W.G., Behre, H.M., Haugen, T.B., Kruger, T., Wang, C., Mbizvo, M.T., and Vogelsong, K.M. (2010). World Health Organization reference values for human semen characteristics. Hum. Reprod. Update *16*, 231–245.
27. Watanabe, S., Kanatsu-Shinohara, M., Ogonuki, N., Matoba, S., Ogura, A., and Shinohara, T. (2018). In vivo genetic manipulation of spermatogonial stem cells and their microenvironment by adeno-associated viruses. Stem Cell Rep. *10*, 1551–1564.
28. Gould, K.G., and Mann, D.R. (1988). Comparison of electrostimulation methods for semen recovery in the rhesus monkey (*Macaca mulatta*). J. Med. Primatol. *17*, 95–103.
29. National Research Council (U.S.). Committee for the Update of the Guide for the Care and Use of Laboratory Animals., Institute for Laboratory Animal Research (U.S.), and National

Academies Press (U.S.). (2011). Guide for the Care and Use of Laboratory Animals. In. (Washington, D.C., National Academies Press)xxv, 220 p.
30. Bolger, A.M., Lohse, M., and Usadel, B. (2014). Trimmomatic: a flexible trimmer for Illumina sequence data. Bioinformatics *30*, 2114–2120.
31. Kim, D., Langmead, B., and Salzberg, S.L. (2015). HISAT: a fast spliced aligner with low memory requirements. Nat. Methods *12*, 357–360.
32. Langmead, B., and Salzberg, S.L. (2012). Fast gapped-read alignment with Bowtie 2. Nat. Methods *9*, 357–359.
33. Roberts, A., and Pachter, L. (2013). Streaming fragment assignment for real-time analysis of sequencing experiments. Nat. Methods *10*, 71–73.
34. Anders, S., McCarthy, D.J., Chen, Y., Okoniewski, M., Smyth, G.K., Huber, W., and Robinson, M.D. (2013). Count-based differential expression analysis of RNA sequencing data using R and Bioconductor. Nat. Protoc. *8*, 1765–1786.
35. Kanehisa, M., Araki, M., Goto, S., Hattori, M., Hirakawa, M., Itoh, M., Katayama, T., Kawashima, S., Okuda, S., Tokimatsu, T., and Yamanishi, Y. (2008). KEGG for linking genomes to life and the environment. Nucleic Acids Res. *36*, D480–D484.
36. Love, M.I., Huber, W., and Anders, S. (2014). Moderated estimation of fold change and dispersion for RNA-seq data with DESeq2. Genome Biol. *15*, 550.
37. Liu, C., He, X., Liu, W., Yang, S., Wang, L., Li, W., Wu, H., Tang, S., Ni, X., Wang, J., et al. (2019). Bi-allelic mutations in TTC29 cause male subfertility with asthenoteratospermia in humans and mice. Am. J. Hum. Genet. *105*, 1168–1181.
38. Lu, S., Wang, J., Chitsaz, F., Derbyshire, M.K., Geer, R.C., Gonzales, N.R., Gwadz, M., Hurwitz, D.I., Marchler, G.H., Song, J.S., et al. (2020). CDD/SPARCLE: the conserved domain database in 2020. Nucleic Acids Res. *48*, D265–D268.
39. Auger, J., Jouannet, P., and Eustache, F. (2016). Another look at human sperm morphology. Hum. Reprod. *31*, 10–23.
40. Li, C.H., Yan, L.Z., Ban, W.Z., Tu, Q., Wu, Y., Wang, L., Bi, R., Ji, S., Ma, Y.H., Nie, W.H., et al. (2017). Long-term propagation of tree shrew spermatogonial stem cells in culture and successful generation of transgenic offspring. Cell Res. *27*, 241–252.
41. Cao, J., Yang, E.B., Su, J.J., Li, Y., and Chow, P. (2003). The tree shrews: adjuncts and alternatives to primates as models for biomedical research. J. Med. Primatol. *32*, 123–130.
42. Zhang, Y.E., Vibranovski, M.D., Landback, P., Marais, G.A.B., and Long, M. (2010). Chromosomal redistribution of male-biased genes in mammalian evolution with two bursts of gene gain on the X chromosome. PLoS Biol. *8*, e1000494.
43. Vinckenbosch, N., Dupanloup, I., and Kaessmann, H. (2006). Evolutionary fate of retroposed gene copies in the human genome. Proc. Natl. Acad. Sci. USA *103*, 3220–3225.
44. Thauvin-Robinet, C., Lee, J.S., Lopez, E., Herranz-Pérez, V., Shida, T., Franco, B., Jego, L., Ye, F., Pasquier, L., Loget, P., et al. (2014). The oral-facial-digital syndrome gene C2CD3 encodes a positive regulator of centriole elongation. Nat. Genet. *46*, 905–911.
45. Obholz, K.L., Akopyan, A., Waymire, K.G., and MacGregor, G.R. (2006). FNDC3A is required for adhesion between spermatids and Sertoli cells. Dev. Biol. *298*, 498–513.
46. Rao, S., Amorim, R., Niu, M., Temzi, A., and Mouland, A.J. (2018). The RNA surveillance proteins UPF1, UPF2 and SMG6 affect HIV-1 reactivation at a post-transcriptional level. Retrovirology *15*, 42.
47. MacDonald, C.C., and Grozdanov, P.N. (2017). Nonsense in the testis: multiple roles for nonsense-mediated decay revealed in male reproduction. Biol. Reprod. *96*, 939–947.
48. Wambergue, C., Zouari, R., Fourati Ben Mustapha, S., Martinez, G., Devillard, F., Hennebicq, S., Satre, V., Brouillet, S., Halouani, L., Marrakchi, O., et al. (2016). Patients with multiple morphological abnormalities of the sperm flagella due to DNAH1 mutations have a good prognosis following intracytoplasmic sperm injection. Hum. Reprod. *31*, 1164–1172.
49. Liu, C., Miyata, H., Gao, Y., Sha, Y., Tang, S., Xu, Z., Whitfield, M., Patrat, C., Wu, H., Dulioust, E., et al. (2020). Bi-allelic DNAH8 variants lead to multiple morphological abnormalities of the sperm flagella and primary male infertility. Am. J. Hum. Genet. *107*, 330–341.

The American Journal of Human Genetics, Volume *110*

Supplemental information

Deficiency of primate-specific *SSX1* induced asthenoteratozoospermia in infertile men and cynomolgus monkey and tree shrew models

Chunyu Liu, Wei Si, Chaofeng Tu, Shixiong Tian, Xiaojin He, Shengnan Wang, Xiaoyu Yang, Chencheng Yao, Cong Li, Zine-Eddine Kherraf, Maosen Ye, Zixue Zhou, Yuhua Ma, Yang Gao, Yu Li, Qiwei Liu, Shuyan Tang, Jiaxiong Wang, Hexige Saiyin, Liangyu Zhao, Liqun Yang, Lanlan Meng, Bingbing Chen, Dongdong Tang, Yiling Zhou, Huan Wu, Mingrong Lv, Chen Tan, Ge Lin, Qingpeng Kong, Hong Shi, Zhixi Su, Zheng Li, Yong-Gang Yao, Li Jin, Ping Zheng, Pierre F. Ray, Yue-Qiu Tan, Yunxia Cao, and Feng Zhang

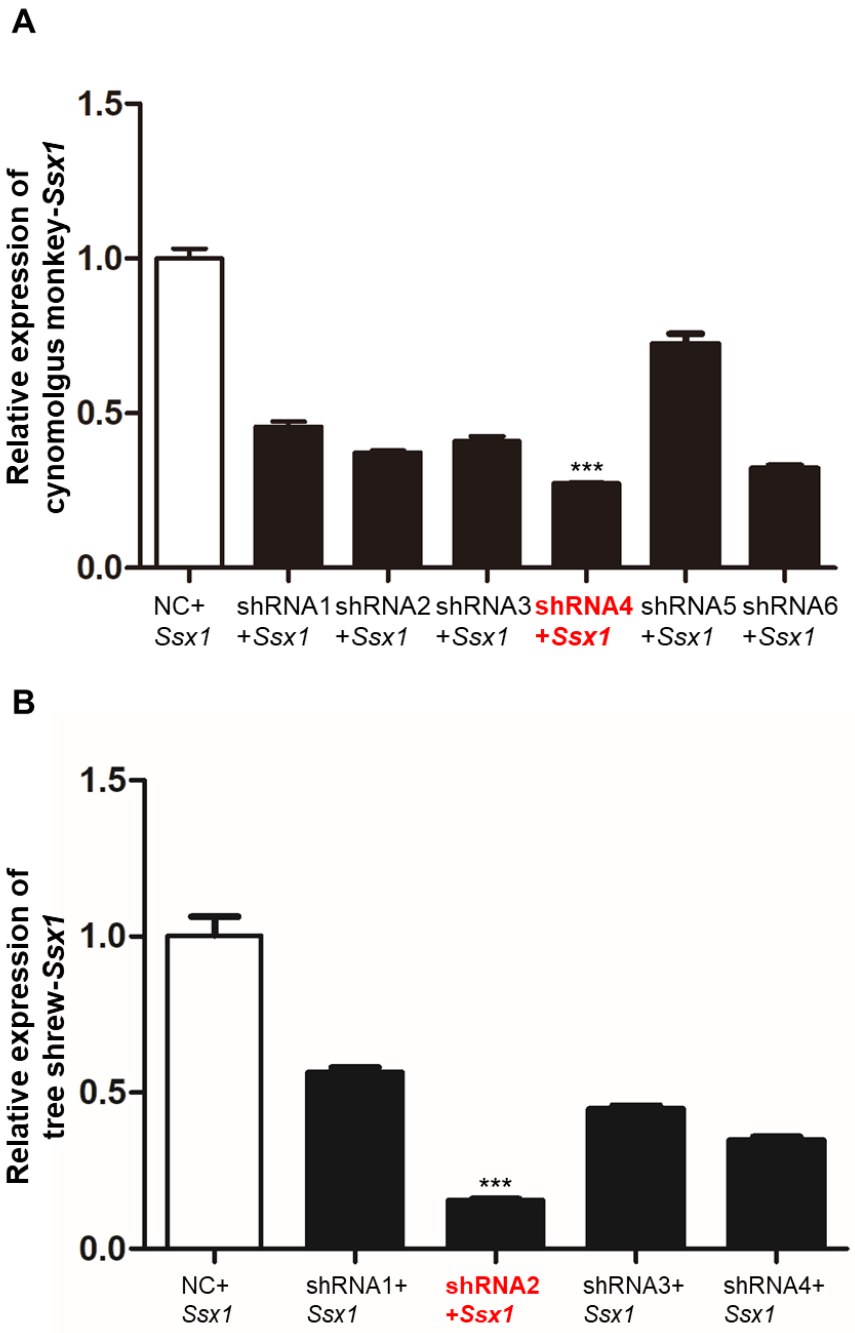

Figure S1. RT-qPCR analysis of knockdown efficacy for *Ssx1* by different shRNAs of cynomolgus monkey (A) and tree shrew (B). Data represent the means ± standard error of measurement (SEM) of three independent experiments. Two-tailed Student's paired or unpaired *t* tests were used as appropriate (***$P < 0.001$). NC, negative control.

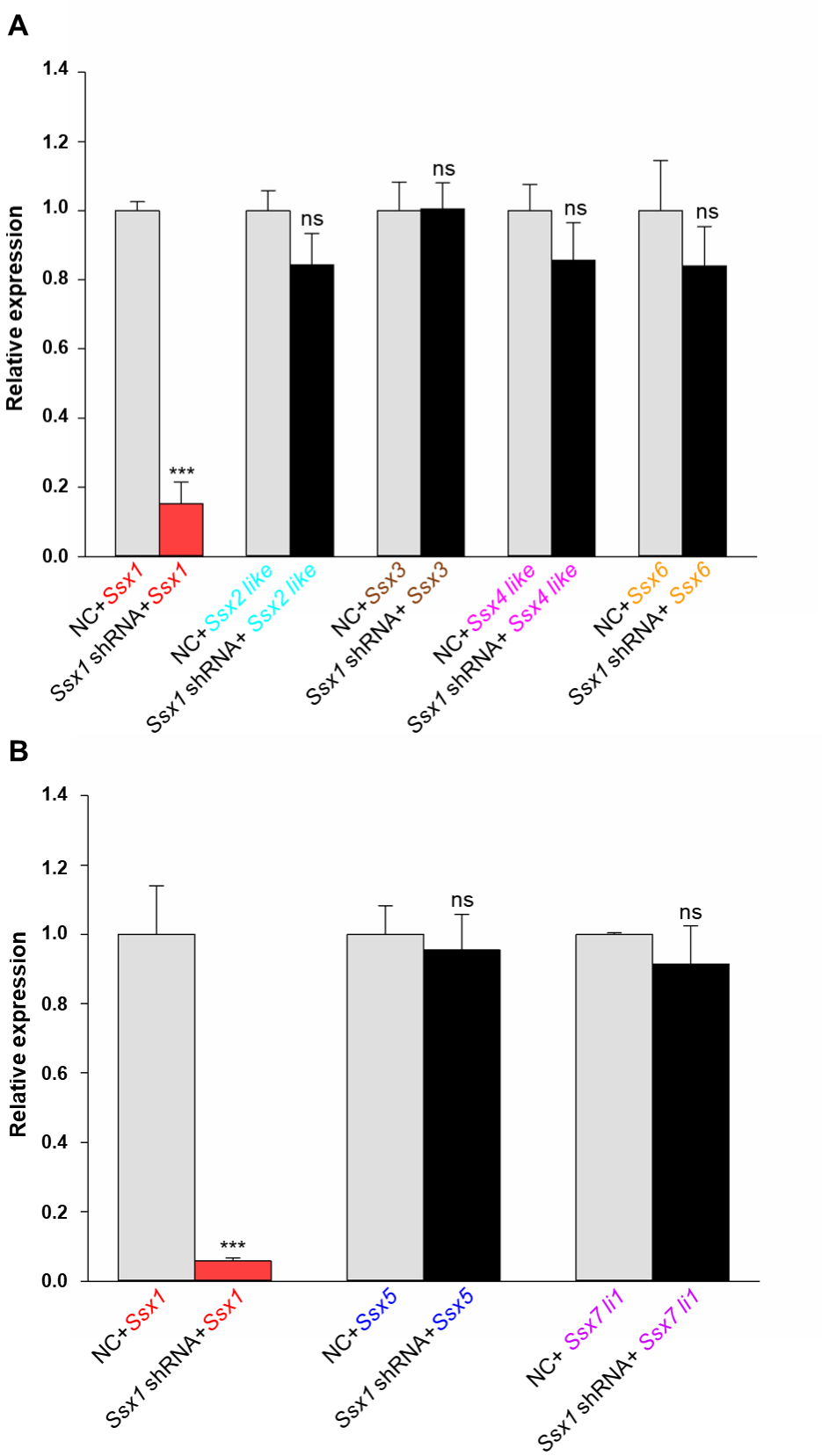

Figure S2. RT-qPCR analysis indicated the significantly reduced expressions of *Ssx1* in cynomolgus monkey (A) and tree shrew (B) models. Data represent the means ± standard error of measurement (SEM) of three independent experiments. Two-tailed Student's paired or unpaired *t* tests were used as appropriate (*** $P < 0.001$).

A

WT

Donor site predictions for NG_012528.2:5031-17083 :

Start	End	Score	Exon	Intron
9	23	0.94	aaaattg	gtgagaat
77	91	1.00	aaacaag	gtatgcct
121	135	0.51	aaaggag	gtatcggt
139	153	0.98	tgttccc	gtaagtga
151	165	0.71	tgaagag	gttggtaa
493	507	0.97	taactcc	gtaagtga
718	732	0.97	accccag	gtcagccc

***SSX1* splice-site mutation c.*4+1G>A**

Donor site predictions for NG_012528.2:5031-17083 :

Start	End	Score	Exon	Intron
9	23	0.94	aaaattg	gtgagaat
77	91	1.00	aaacaag	gtatgcct
121	135	0.51	aaaggag	gtatcggt
139	153	0.98	tgttccc	gtaagtga
151	165	0.71	tgaagag	gttggtaa
718	732	0.97	accccag	gtcagccc

B

variant	gene	Δ type	Δ score ⓘ	pre-mRNA position ⓘ
X-48125827-G-A UCSC, gnomAD	SSX1 (ENSG00000126752.8_1 / ENST00000376919.4_1 / NM_005635.4, NM_001278691.2) biotype: protein coding canonical transcript OMIM, GTEx, gnomAD, ClinGen, Ensembl, Decipher, GeneCards	Acceptor Loss	0.00	
		Donor Loss	1.00	-1 bp
		Acceptor Gain	0.00	
		Donor Gain	0.01	3 bp

C

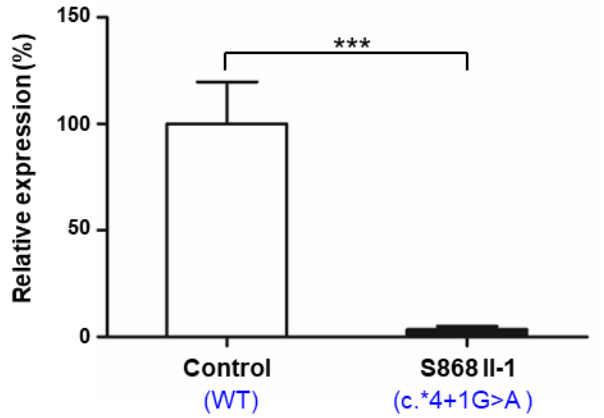

Figure S3. The effect of the mutated site (c.*4+1G>A) on the splicing of *SSX1* mRNA.

(A) A prediction for *SSX1* c.*4+1G>A using the online tool of Splice Site Prediction by Neural Network (NNSPLICE 0.9) at http://www.fruitfly.org/seq_tools/splice.html. The red box represents the missing donor site caused by the splicing variant c.*4+1G>A in *SSX1*.

(B) A prediction for *SSX1* c.*4+1G>A using the SpliceAI tool (a 32-layer deep neural network to predict splicing from a pre-mRNA sequence; https://spliceailookup.broadinstitute.org/). The delta score higher than 0.8 indicated the prediction of a donor loss with high precision.

(C) Expression analysis of *SSX1* in the spermatozoa from men harboring the hemizygous splicing variant c.*4+1G>A in *SSX1*. The primers used for RT-qPCR assay were designed between exons 4 and 6 of *SSX1* (Transcript ID: ENST00000376919.3). Data represent the means ± standard error of measurement (SEM) of three independent experiments. Two-tailed Student's paired or unpaired *t* test was used as appropriate (***$P < 0.001$).

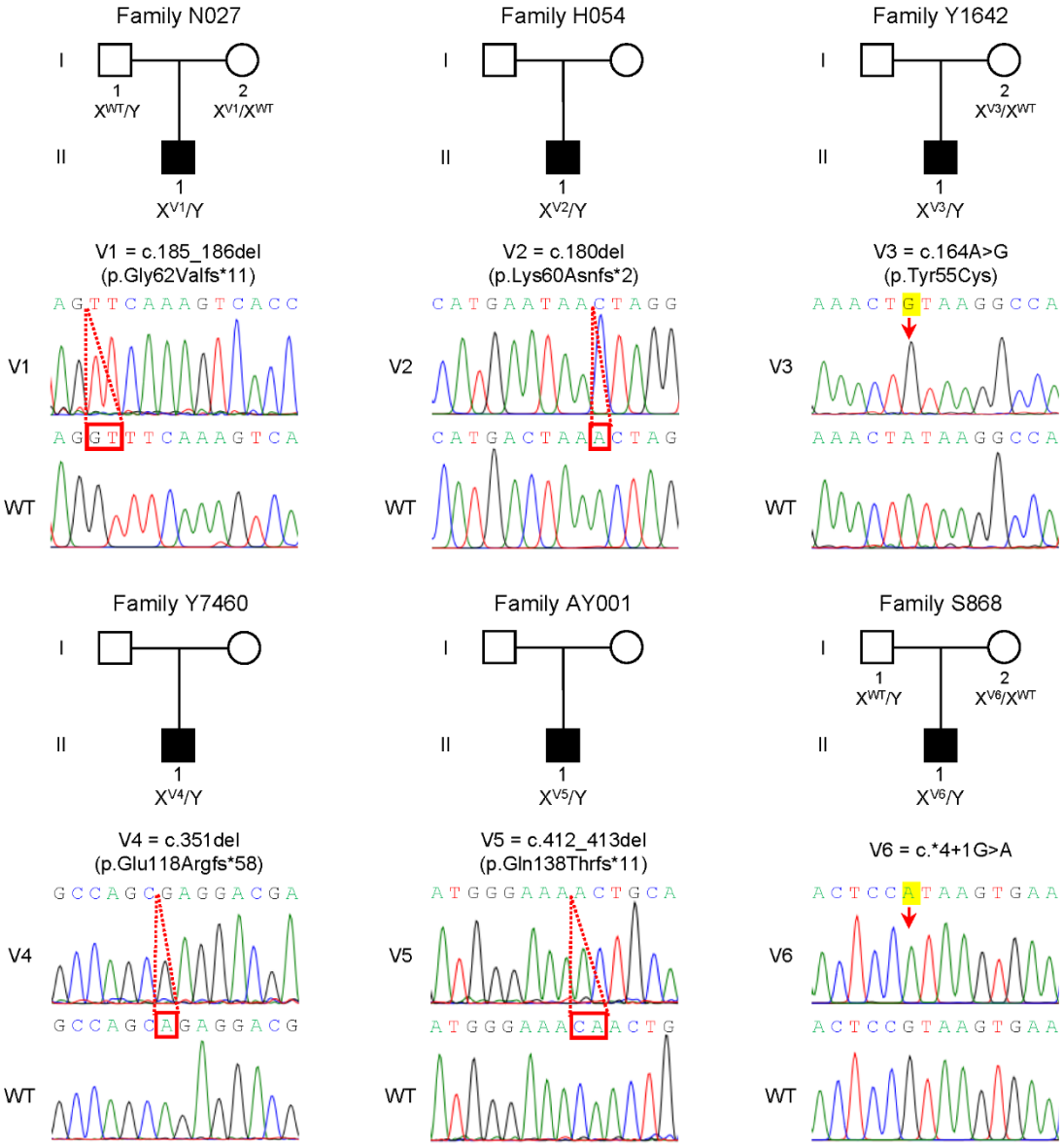

Figure S4. Sanger sequencing confirmed hemizygous *SSX1* variants (V1–V6) in infertile men N027 II-1, H054 II-1, Y1642 II-1, Y7460 II-1, AY001 II-1 and S868 II-1.

The positions of the variants are indicated by red arrows or boxes. Abbreviations: V1, variant 1; V2, variant 2; V3, variant 3; V4, variant 4; V5, variant 5; V6, variant 6; WT, wild type.

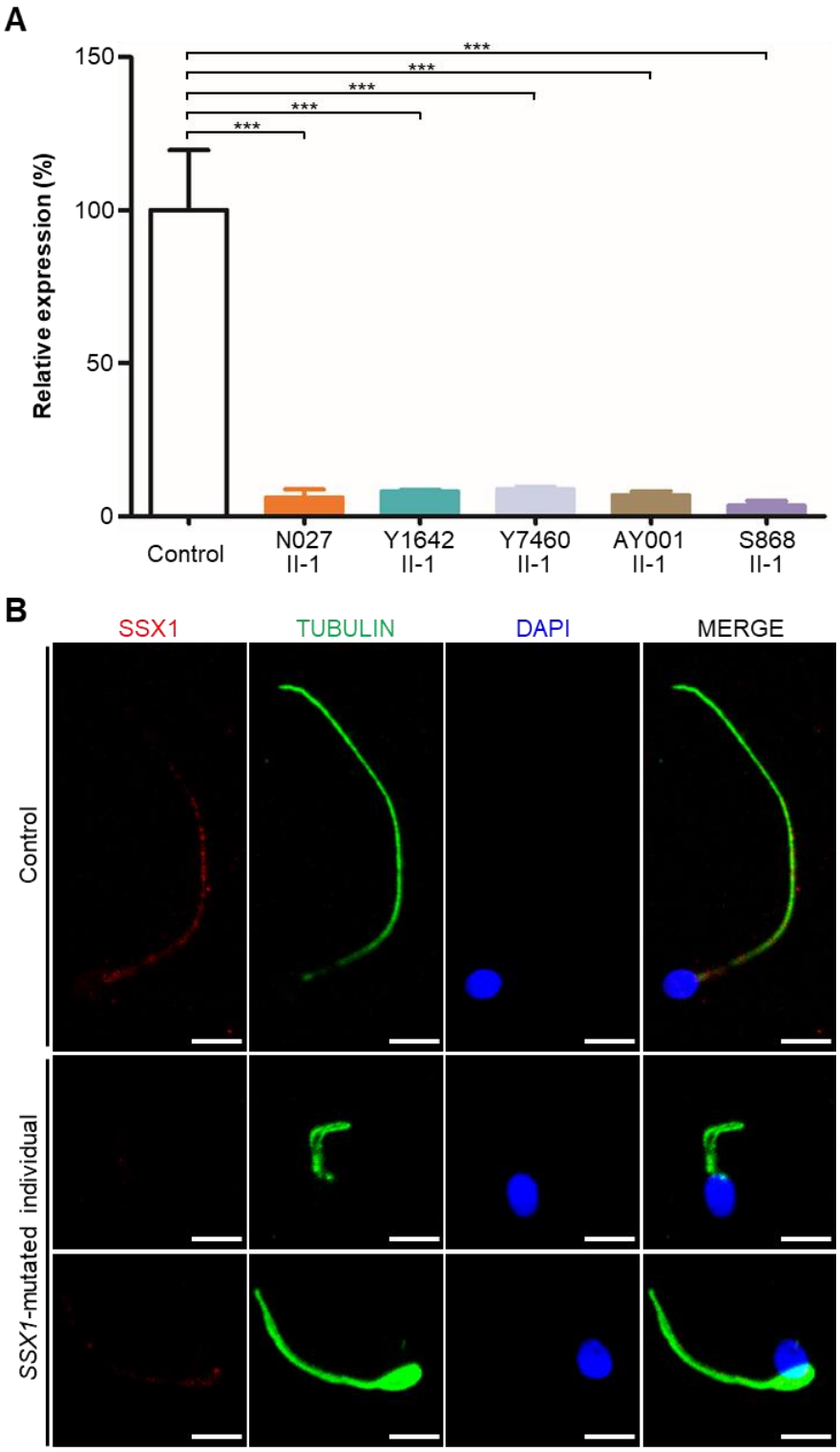

Figure S5. Analysis of *SSX1* mRNA and protein levels in the spermatozoa from a male control and men harboring hemizygous *SSX1* variants.

(A) RT–qPCR analysis indicated that the abundance of *SSX1* mRNA was dramatically reduced in the spermatozoa from men harboring hemizygous *SSX1* variants when compared to that in the spermatozoa from a control male. The data are presented as the mean ± standard error of three independent experiments. Two-tailed Student's paired or unpaired *t* tests were used as appropriate (***$P < 0.001$).

(B) IF staining of SSX1 in the spermatozoa from a male control individual and men harboring hemizygous *SSX1* variants. SSX1 staining (red) is concentrated at the midpiece and principal piece of sperm flagella from the control individual but absent in the sperm flagella from men harboring hemizygous *SSX1* variants. Sperm flagella were stained with anti-α-tubulin (green) antibodies, and DNA was counterstained with DAPI as a nuclear marker. Scale bars: 5 μm. The data of subject N027 II-1 were used as an example.

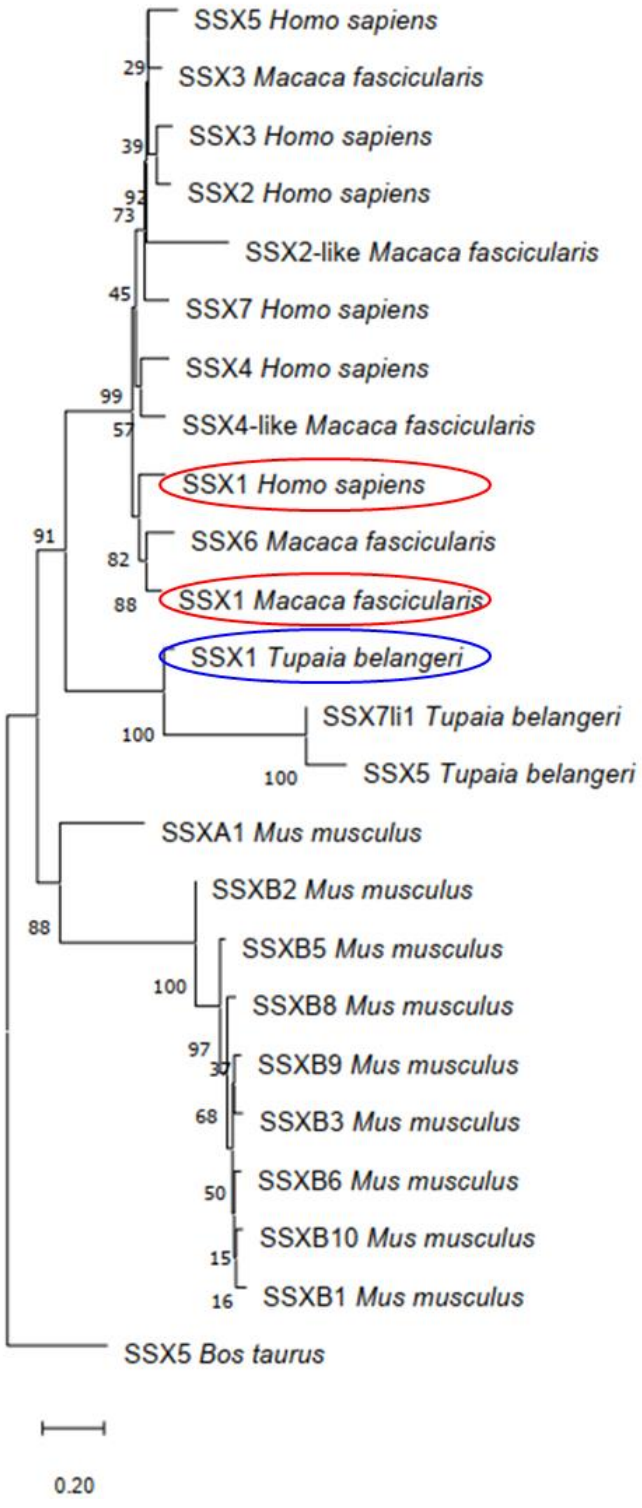

Figure S6. Phylogenetic tree of SSX family members from mouse (*Mus musculus*), tree shrew (*Tupaia belangeri*), cynomolgus monkey (*Macaca fascicularis*) and human (*Homo sapiens*) with the Neighbor-Joining algorithm using *Bos taurus* SSX5 as an outgroup. The percentages of replicate trees in which the associated taxa clustered together in the bootstrap test (1000 replicates) are shown next to the branches. The tree is drawn to scale, with branch lengths in the same units as those of the evolutionary distances used to infer the phylogenetic tree.

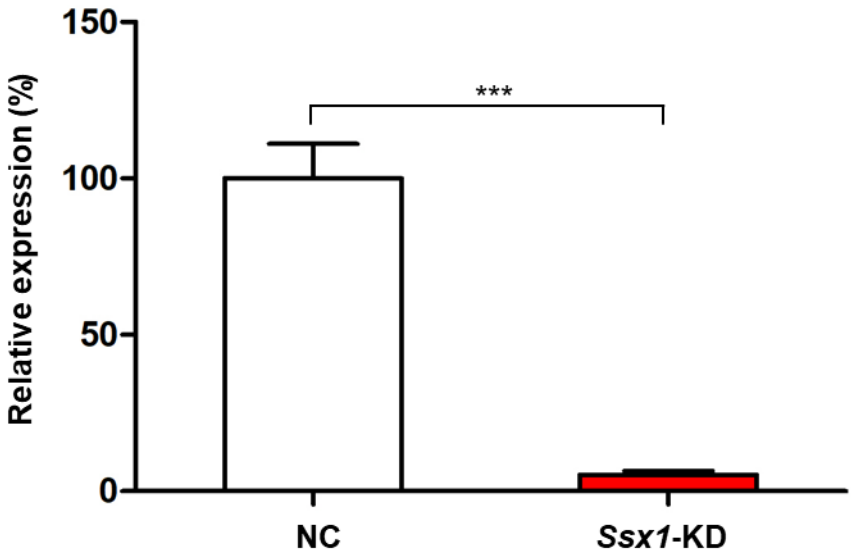

Figure S7. Expression analysis of *Ssx1* mRNA in the testes of negative control (NC) and *Ssx1*-KD male cynomolgus monkeys.

RT-qPCR analysis indicated that the abundance of *Ssx1* mRNA was dramatically reduced in the testes of *Ssx1*-KD male cynomolgus monkeys when compared to that of NC group. Data represent the means ± SEM of three independent experiments. Two-tailed Student's paired or unpaired *t* test was used as appropriate (***$P < 0.001$).

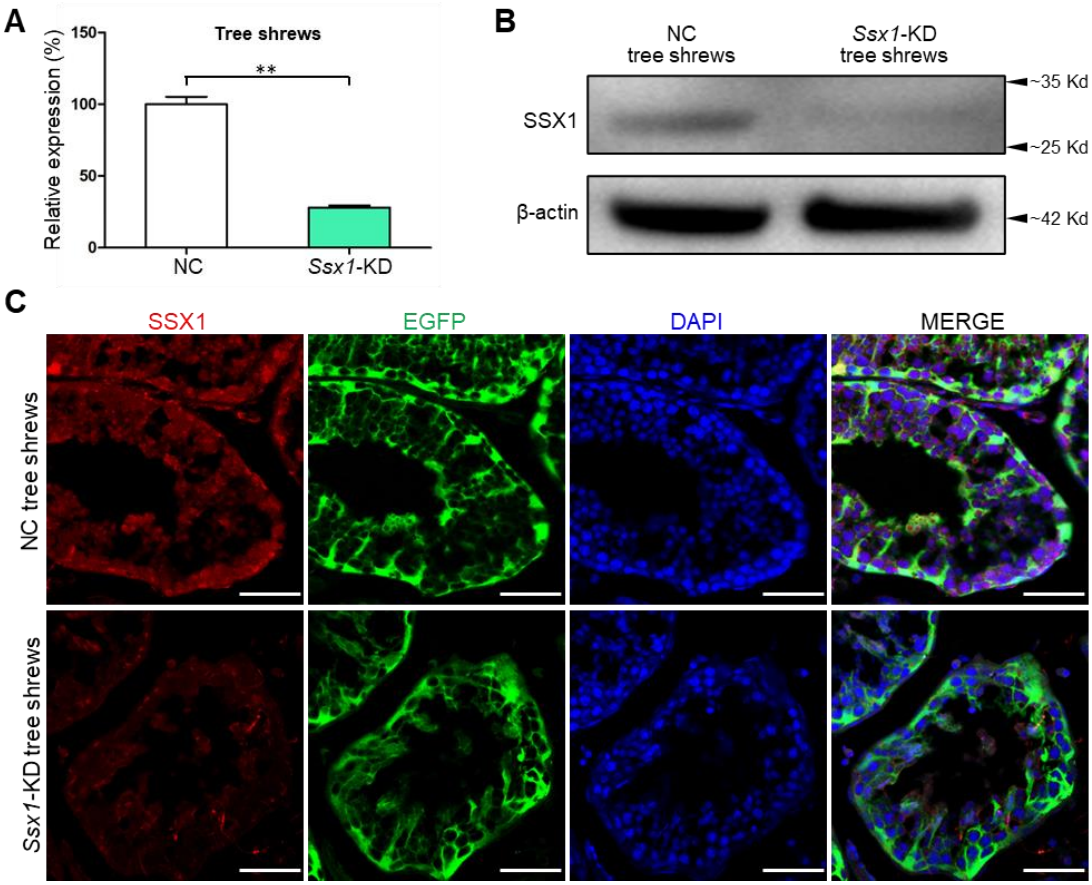

Figure S8. Detection of the efficacy of *Ssx1* expression KD in the testes of adult male tree shrews.
(A) RT–qPCR analysis revealed a significant reduction of *Ssx1* mRNA abundance in the testes of *Ssx1*-KD male tree shrews when compared to that in the testes of negative control (NC) male tree shrews. The data are presented as the mean ± standard error of three independent experiments. Two-tailed Student's paired or unpaired *t* tests were used as appropriate (**$P < 0.01$).
(B) Immunoblotting assays indicated that SSX1 was dramatically reduced in the testes from *Ssx1*-KD male tree shrews. β-actin was used as a loading control.
(C) IF staining of SSX1 in the testes from NC male tree shrews and *Ssx1*-KD male tree shrews. SSX1 immunostaining (red) was mainly concentrated in the spermatogonia or spermatocytes from NC male tree shrews but was dramatically decreased in testicular sections from *Ssx1*-KD male tree shrews. DNA was counterstained with DAPI as a nuclear marker. Scale bars: 50 μm.

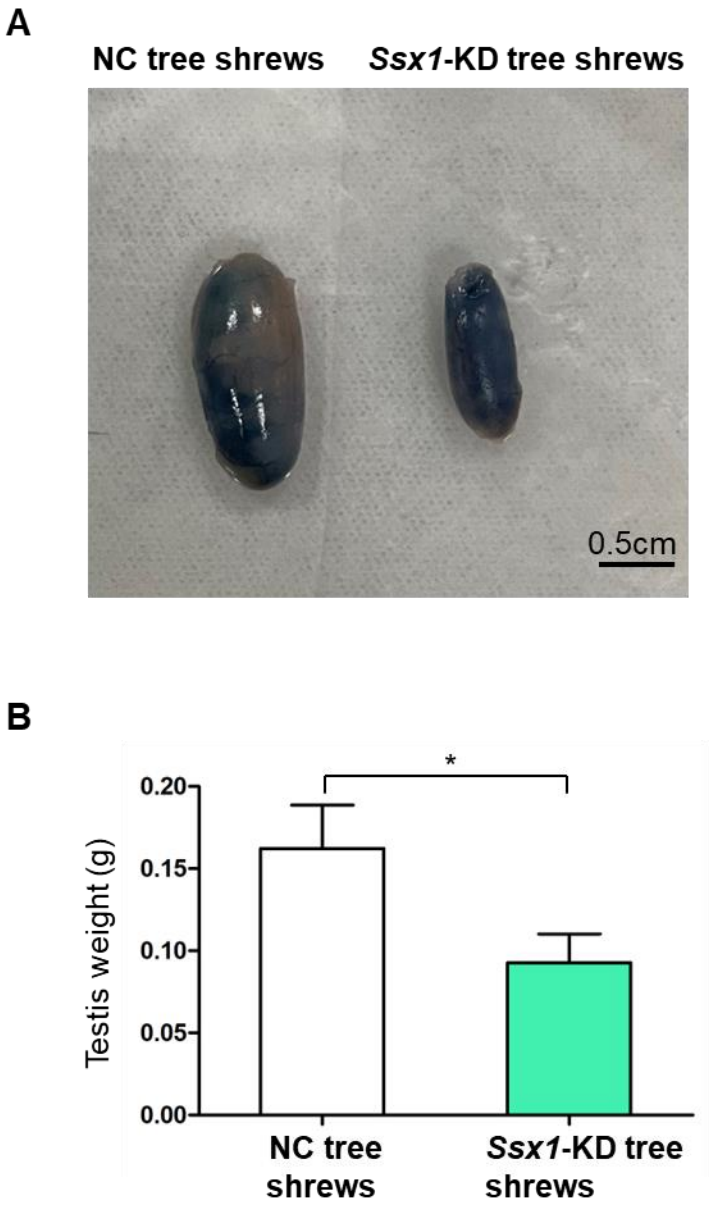

Figure S9. Testis sizes and weights in negative control (NC) and *Ssx1*-KD male tree shrews.
(A) Testis sizes in tree shrew models.
(B) Reduced testis weights were observed in *Ssx1*-KD male tree shrews when compared to those in NC group. For each group, at least five tree shrews were counted and the data represent the means ± SEM; **P* < 0.05.

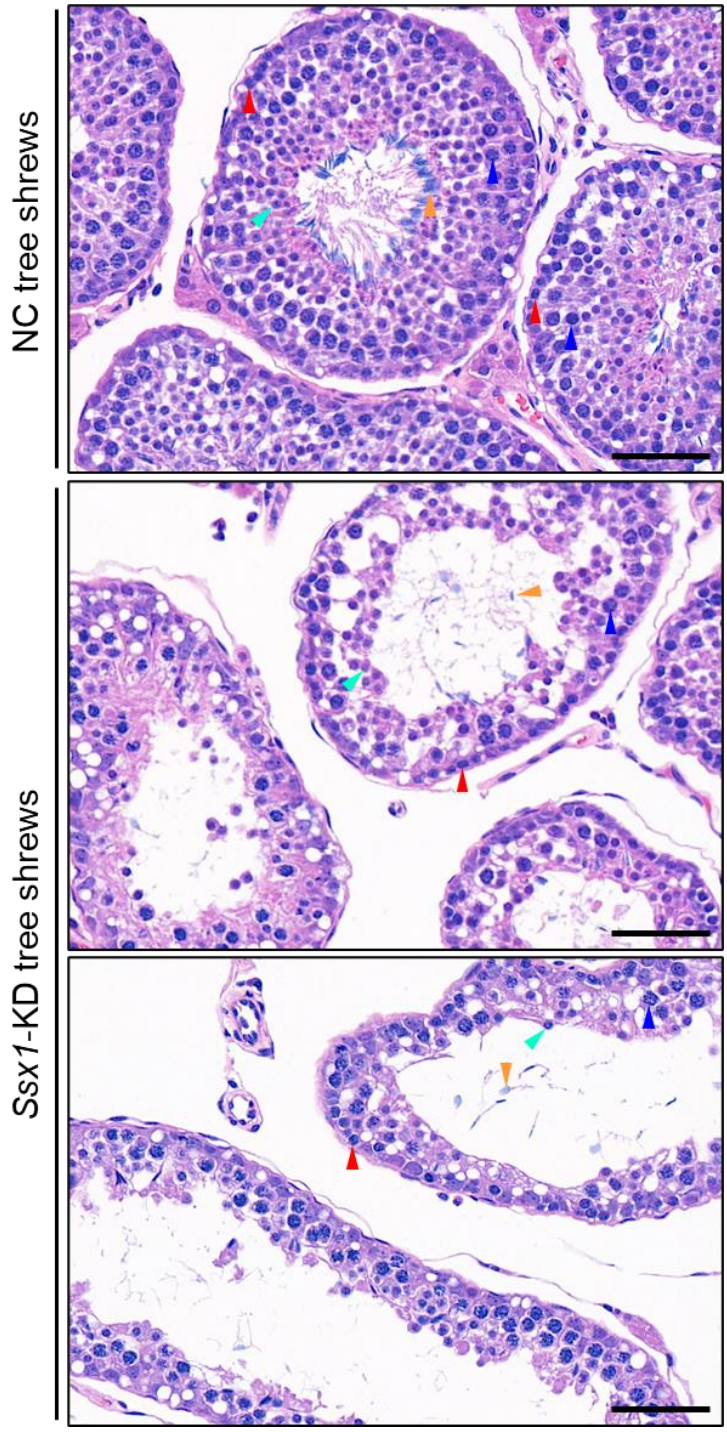

Figure S10. H&E staining of testicular tissue sections obtained from *Ssx1*-KD male tree shrews. All germ cells were regularly arranged in the seminiferous epithelia of negative control (NC) male tree shrews but displayed a loss or disordered arrangement in the testes from *Ssx1*-KD male tree shrews; spermatogonia (red arrowheads), spermatocytes (dark blue arrowheads), round spermatids (light blue arrowheads) and spermatozoa (orange arrowheads). Scale bars: 50 μm.

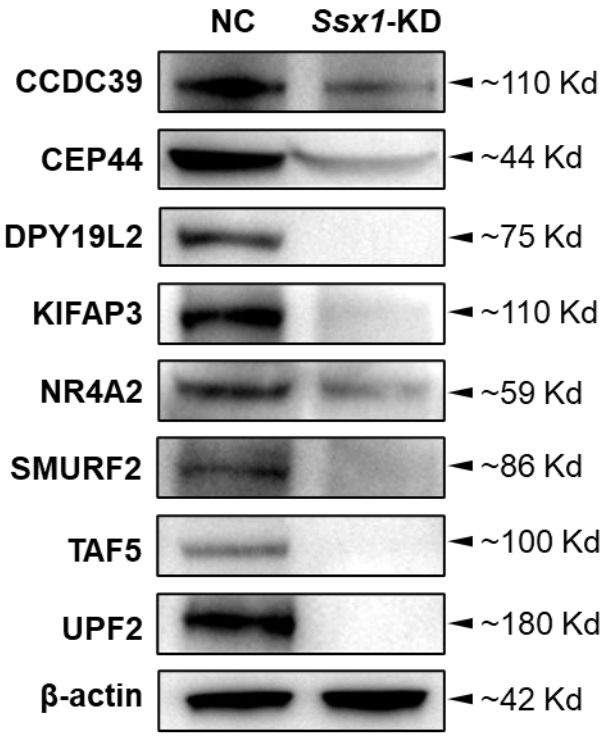

Figure S11. **Western blotting assay revealed significantly reduced levels of multiple selected proteins in the testes from *Ssx1*-KD tree shrews**. β-actin was used as a loading control. NC, negative control.

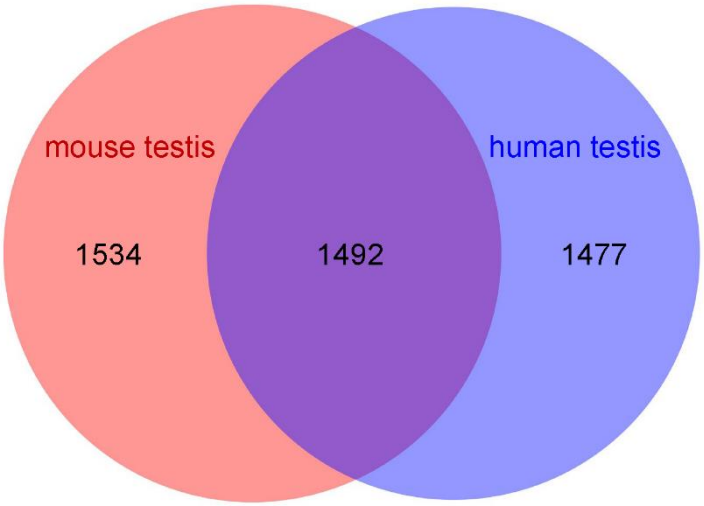

Figure S12. Analysis of the evolutionary divergence of human and mouse testis-enriched genes. The number "1492" represents the number of testis-enriched genes that are evolutionarily conserved between human and mouse. The number "1477" represents the number of human-specific testis-enriched genes, which do not have one-to-one orthologs in mouse or the mouse orthologs of which are not testis-enriched. The number "1534" represents the number of mouse-specific testis-enriched genes, which do not have one-to-one orthologs in human or the human orthologs of which are not testis-enriched.

Primer name	Primer sequence (5'-3')	Tm
V1-F	CAATCCTTCTGCCCAGCCG	56°C
V1-R	AGGTAGCTGAGCTGAAAAGCAAT	
V2-F	AGGCCTTTGATGATATTGCCAC	56°C
V2-R	CCACAGAGACAGCTGGGCTG	
V3-F	TTCTGAGGAGGGGAGGAC	52°C
V3-R	AAAGGAAAATGTGGGGTA	
V4-F	TGTTTTGTCCCCTCCCTA	53°C
V4-R	AGAATCGCTTGAGCACCT	
V5-F	GTCCCCTCCCTATGTTTT	50°C
V5-R	GATTTAATTTAATGCCTCC	
V6-F	AGGTTGGTAATCTAAACGTC	50°C
V6-R	CCACTGCCCAATAACTCA	

Table S1. Primers used for amplification and verification of *SSX1* variants

Species and locus	Sequence (5'-3')
Cynomolgus monkey-shNC	Top strand: gatccgTTCTCCGAACGTGTCACGTAAttcaagagaTTACGTGAC ACGTTCGGAGAAttttttc
	Bottom strand: aattgaaaaaaTTCTCCGAACGTGTCACGTAAtctcttgaaTTACGTG ACACGTTCGGAGAAcg
Cynomolgus monkey-sh*Ssx1*	Top strand: aattcGCCACAGGAATCAGGTTGAACGTCCTttcaagagaAGGA CGTTCAACCTGATTCCTGTGGttttttg
	Bottom strand: gatccaaaaaaCCACAGGAATCAGGTTGAACGTCCTtctcttgaaAG GACGTTCAACCTGATTCCTGTGGCg
Tree shrew-shNC	Top strand: gatccgTTCTCCGAACGTGTCACGTAAttcaagagaTTACGTGAC ACGTTCGGAGAAttttttc
	Bottom strand: aattgaaaaaaTTCTCCGAACGTGTCACGTAAtctcttgaaTTACGTG ACACGTTCGGAGAAcg
Tree shrew-sh*Ssx1*	Top strand: aattcGCCTTCAACGATATTTCCAAATACTttcaagagaAGTATT TGGAAATATCGTTGAAGGCttttttg
	Bottom strand: gatccaaaaaaGCCTTCAACGATATTTCCAAATACTtctcttgaaAG TATTTGGAAATATCGTTGAAGGCg

Table S2. Sequences of the shRNAs used for knocking down *Ssx1* in male cynomolgus monkeys and tree shrews

Uppercase and lowercase letters indicate the siRNA sequence and shRNA skeleton, respectively, for each shRNA.

Primer name	Primer sequence (5'-3')	Tm
Human-*SSX1*-F	TCACCCTCCCACCTTTCA	60°C
Human-*SSX1*-R	TCGTCCTCTGCTGGCTTC	
Human-*GAPDH*-F	GGAGCGAGATCCCTCCAAAAT	60°C
Human-*GAPDH*-R	GGCTGTTGTCATACTTCTCATGG	
Monkey-*Ssx1*-F	ACCGTAACCACAGGAATC	60°C
Monkey-*Ssx1*-R	ATCTTCTCAGAGGTATTTGC	
Monkey-*actin*-F	ACGTGGACATCCGTAAAG	60°C
Monkey-*actin*-R	GGGCCAGACTCGTCATAC	
Tree shrew-*Ssx1*-F	CCGCAGAAAAGACACTCG	60°C
Tree shrew-*Ssx1*-R	CGGCACGGTAGTTTGGAG	
Tree shrew-*actin*-F	ATTTTGAATGATCAGCCACC	58°C
Tree shrew-*actin*-R	AGGTAAGCCCTGGCTGCCTC	

Table S3. Primers used for RT-qPCR assays

Primer name	Primer sequence (5'-3')	Tm
TS-*Alms1* F	AAAGGCAGTGACTAAGGTT	49°C
TS-*Alms1* R	GACAGAATGAGTAGTATTTTCG	
TS-*Cep44* F	AGAATGACTTGCGCTTTA	48°C
TS-*Cep44* R	ACTACTGAGTTCCTTGTGCT	
TS-*Cep170* F	AAGTGCCAAAAGCATAGA	50°C
TS-*Cep170* R	CATCCACCTCATCATCCC	
TS-*C2cd3* F	TCAAAACGGATGGAAAAG	51°C
TS-*C2cd3* R	TCCTTGGTAGGTGGGTTA	
TS-*Ccdc39* F	CATTGGAAGCCTGGTTAG	50°C
TS-*Ccdc39* R	TACGAAAATCCTGTGCTG	
TS-*Cep164* F	TGACGAACACTATCGGAACT	53°C
TS-*Cep164* R	CGCTTCTAGCCTGCATCT	
TS-*Cfap58* F	ATCAAAAGGCAGAAGTGG	58°C
TS-*Cfap58* R	TATCTGTTTCTGGGTCGC	
TS-*Cmtr2* F	CAAAGGGTACTTCAATAGTTG	49°C
TS-*Cmtr2* R	ATGGAGACAGAAAACGGA	
TS-*Dpy19l2* F	AGCCTCTGAGCCAAGTGC	53°C
TS-*Dpy19l2* R	CGAGGAATGGGTAGGAGA	
TS-*Fndc3a* F	ACCTGGTTTTATTCCTGTC	49°C
TS-*Fndc3a* R	GTGATGATGGTGGACTGC	
TS-*Ica1l* F	GCACGCACGGAATACAGA	55°C
TS-*Ica1l* R	TCCCAGAATCCGAGCAGT	
TS-*Iqce* F	TTTCCACAAACCTCCACC	53°C
TS-*Iqce* R	ACGCCTGAGATTTGACCT	
TS-*Kifap3* F	ACAAGCCTAAAGACCCAC	49°C
TS-*Kifap3* R	TCAACACTCTGTTTCCAGTC	
TS-*Lrrcc1* F	AGAAGACCGAAATCATTAA	48°C
TS-*Lrrcc1* R	TTTTAGCCTGTCTGTGGTA	
TS-*Nr4a2* F	CGCACATGATCGAGCAGA	57°C
TS-*Nr4a2* R	GTTGGGCACAGCGAAGGT	
TS-*Smurf2* F	TCCTCCAGACCTACCAGA	49°C
TS-*Smurf2* R	ATTACGAATCTCCCATCC	
TS-*Taf5* F	GATGGTGGGAAGTTTGGC	54°C
TS-*Taf5* R	GCGTACTCGTTTGGTGGT	
TS-*Ttll10* F	GCCCATTCTTCTACATCG	52°C
TS-*Ttll10* R	CACTTGACCTCGCACCAT	
TS-*Upf2* F	TTTCCTCCAAGTGAAATAA	47°C
TS-*Upf2* R	ATCCAAAAGGTCTGCTAA	
TS-*Usp1* F	AATAAGCAACCCAGCATT	52°C
TS-*Usp1* R	ACATTCCAAGCAGCGAGT	
TS-*Usp47* F	ATTTACCAGCATCTACTCCA	49°C
TS-*Usp47* R	GAACACTATCGTCTACAGCA	
TS-*Wdpcp* F	AACTGGGATACTATGGGC	50°C
TS-*Wdpcp* R	CAGAAGTGGTCTTGTGGG	

Table S4. Primers used for the verification of RNA-seq assays